

## Exploring *Klebsiella pneumoniae* capsule polysaccharide proteins to design multiepitope subunit vaccine to fight against pneumonia

Jyotirmayee Dey, Soumya Ranjan Mahapatra, S Lata, Shubhransu Patro, Namrata Misra & Mrutyunjay Suar

To cite this article: Jyotirmayee Dey, Soumya Ranjan Mahapatra, S Lata, Shubhransu Patro, Namrata Misra & Mrutyunjay Suar (2022): Exploring *Klebsiella pneumoniae* capsule polysaccharide proteins to design multiepitope subunit vaccine to fight against pneumonia, Expert Review of Vaccines, DOI: [10.1080/14760584.2022.2021882](https://doi.org/10.1080/14760584.2022.2021882)

To link to this article: <https://doi.org/10.1080/14760584.2022.2021882>



View supplementary material [↗](#)



Published online: 04 Jan 2022.



Submit your article to this journal [↗](#)



Article views: 27



View related articles [↗](#)



View Crossmark data [↗](#)

ORIGINAL RESEARCH



## Exploring *Klebsiella pneumoniae* capsule polysaccharide proteins to design multiepitope subunit vaccine to fight against pneumonia

Jyotirmayee Dey <sup>a</sup>, Soumya Ranjan Mahapatra <sup>a</sup>, S Lata<sup>b</sup>, Shubhransu Patro<sup>c</sup>, Namrata Misra <sup>a,d</sup> and Mrutyunjay Suar<sup>a,d</sup>

<sup>a</sup>School of Biotechnology, Kalinga Institute of Industrial Technology (KIIT), Deemed to Be University, Bhubaneswar, India; <sup>b</sup>Kalinga Institute of Dental Sciences, KIIT Deemed to Be University, Bhubaneswar, India; <sup>c</sup>Kalinga Institute of Medical Sciences, KIIT Deemed to Be University, Bhubaneswar, India; <sup>d</sup>KIIT-Technology Business Incubator (KIIT-TBI), Kalinga Institute of Industrial Technology (KIIT), Deemed to Be University, Bhubaneswar, India

### ABSTRACT

**Background:** *Klebsiella pneumoniae* is an emerging human pathogen causing neonatal lung disease, catheter-associated infections, and nosocomial outbreaks with high fatality rates. Capsular polysaccharide (CPS) protein plays a major determinant in virulence and is considered as a promising target for vaccine development.

**Research Design and Methods:** In this study, we used immunoinformatic approaches to design a multi-peptide vaccine against *K. pneumoniae*. The epitopes were selected through several immune filters, such as antigenicity, conservancy, nontoxicity, non-allergenicity, binding affinity to HLA alleles, overlapping epitopes, and peptides having common epitopes.

**Results:** Finally, a construct comprising 2 B-Cell, 8 CTL, 2 HTL epitopes, along with adjuvant, linkers was designed. Peptide-HLA interaction analysis showed strong binding of these epitopes with several common HLA molecules. The *in silico* immune simulation and population coverage analysis of the vaccine showed its potential to evoke strong immune responses. Further, the interaction between vaccine and immune was evaluated by docking and simulation, revealing high affinity and complex stability. Codon adaptation and *in silico* cloning revealed higher expression of vaccine in *E. coli* K12 expression system.

**Conclusions:** Conclusively, the findings of the present study suggest that the designed novel multi-epitopic vaccine holds potential for further experimental validation against the pathogen.

### ARTICLE HISTORY

Received 9 April 2021  
Accepted 20 December 2021

### KEYWORDS

*Klebsiella pneumoniae*;  
capsular polysaccharide;  
epitope; vaccine;  
immunoinformatics

## 1. Introduction


*Klebsiella pneumoniae* has been recognized as a causative agent to account for 2 to 5% of community-acquired pneumonia and is the most common cause of lung infections in healthy people [1]. With an estimated 21.7 million pneumonia cases, annually and an even higher number of death cases, the health burden caused by *Klebsiella* is huge [2]. This ubiquitous pathogen still remains an epidemic threat to global public health [3]. *K. pneumoniae* is an encapsulated Gram-negative organism, commensal to the mucosal lining of mammals, human gastrointestinal tract causing nosocomial pneumonia, UTIs, bloodstream infections, pyogenic liver abscess, and metastatic complications [4]. Gastrointestinal symptoms are becoming more widely known among patients, with fever, cough, and shortness of breath are the other common presenting symptoms.

Being a hospital-associated pathogen, *Klebsiella* is continuously exposed to multiple antibiotics resulting in constant selective pressure, which in turn leads to additional mutations that are positively selected. *K. pneumoniae* belongs to the

ESKAPE priority group defined by The World Health Organization (WHO), which also includes *Enterococcus faecium*, *Staphylococcus aureus*, *Acinetobacter baumannii*, *Pseudomonas aeruginosa*, and *Enterobacter spp* [5,6]. The worldwide increase in the occurrence of multi-drug resistant (MDR) *K. pneumoniae* reflects multifactorial dissemination processes that include spread of high-risk global multi-resistant genetic lineages, acquisition of successful multi resistant plasmids; and acquisition of resistance genes located on successful transposons [7,8].

For the removal of *Klebsiella* from human lungs, effective host defense mechanisms are required where the surface of bacteria plays an important role. The three major components of the bacterial outer wall that are said to be triggering the immunity include lipopolysaccharide proteins, outer membrane proteins, and proteoglycans [4,9]. Particularly, acidic Capsular Polysaccharide (CPS), historically known as K-antigen, produced by the bacterium, is the major determinant of virulence, survival, pathogenesis, and antibiotic resistance in *K. pneumoniae*. The polysaccharide capsule is the

**CONTACT** Mrutyunjay Suar  [mrutyunjay@kiitincubator.in](mailto:mrutyunjay@kiitincubator.in); Namrata Misra  [namrata@kiitincubator.in](mailto:namrata@kiitincubator.in)  KIIT School of Biotechnology (KSBT), KIIT University, Campus-11, Patia, Bhubaneswar, Odisha 751024 India

 Supplemental data for this article can be accessed [here](#).

© 2021 Informa UK Limited, trading as Taylor & Francis Group

outermost layer of the cell and protects the bacterium from desiccation, phage, protist predation and can block the phagocytosis [10,11]. Therefore, CPS is considered as a potential target for therapeutic intervention against klebsiella. Reports suggest that biosynthesis of CPS or K-antigen occurring via the Wzx/Wzy-dependent pathway that facilitates the surface expression of CPS can also be a good vaccine/drug target [12,13]. As in this study, the two genes play a vital role in the Wzx/Wzy-dependent pathway hence is highly antigenic for inclusion in vaccine construct. However, till date, no study has been reported to identify potential epitopes from CPS protein as vaccine candidates.

Over the last few decades, various approaches have been tested to combat the pathogenic bacteria and virus through the recent progress in bioinformatics, which has provided novel tools to identify potential drug targets [14,15]. Therefore, this study harnessed the immunoinformatics approach to identify antigenic T-cell (CD8+ & CD4+) and B-cell epitopes on the conserved domains of the CPS protein of *K. pneumoniae*. The top 17 best epitopes of HTL, CTL (CD8<sup>+</sup> cytotoxic T lymphocyte), and B-cell from the CPS proteins, which showed higher immunity, non-allergenicity, nontoxicity, and exhibited higher immunogenicity scores and population coverage were selected for the development of vaccine construct. The epitopes were further linked together using specific linkers. An adjuvant (Cholera Toxin Subunit B) was also added at the N-terminal of the vaccine construct to improve its immunogenicity. Subsequently, the modeled vaccine was subjected to molecular dynamics simulation to confirm the stability of the strong bonding interactions with Toll-like receptor 2. *In silico* cloning was performed to observe the expression of the vaccine. The computer-aided analyses conducted in this

study suggest that the designed multi-epitope vaccine will elicit strong immune responses against *K. pneumoniae*. However, experimental validation is needed to confirm the efficacy of this proposed vaccine candidate.

## 2. Methods and materials

The overall workflow employed for vaccine design is presented in Figure 1.

### 2.1. Vaccine protein prioritization

The sequences of CPS protein (Accession Id: H2CZH6, B5XT46) of the *K. pneumoniae* were collected from UniProt (<https://uniprot.org>) database and its fasta sequences were downloaded to carry out further analysis. Sequence similarity search of the CPS protein was performed to avoid the cross-reactivity and generation of autoimmune disorder against the human proteome by using NCBI-Protein-Protein Blast ([https://blast.ncbi.nlm.nih.gov/Blast.cgi?PROGRAM=blastp&PAGE\\_TYPE=BlastSearch&LINK\\_LOC=blasthome](https://blast.ncbi.nlm.nih.gov/Blast.cgi?PROGRAM=blastp&PAGE_TYPE=BlastSearch&LINK_LOC=blasthome)). Figure 2 illustrates the schematic representation of the immunoinformatic tools used for epitope-based vaccine target identification and design of a promiscuous vaccine construct against *K. pneumoniae*.

### 2.2. Prediction of T-cell

The T-cell epitopes are typically peptide fragments (containing 12 to 20 amino acids) that are immunodominant and can elicit specific immune responses, and therefore important for epitope-based peptide vaccine design. Effective immune response depends on the specificity and diversity of the antigen-binding

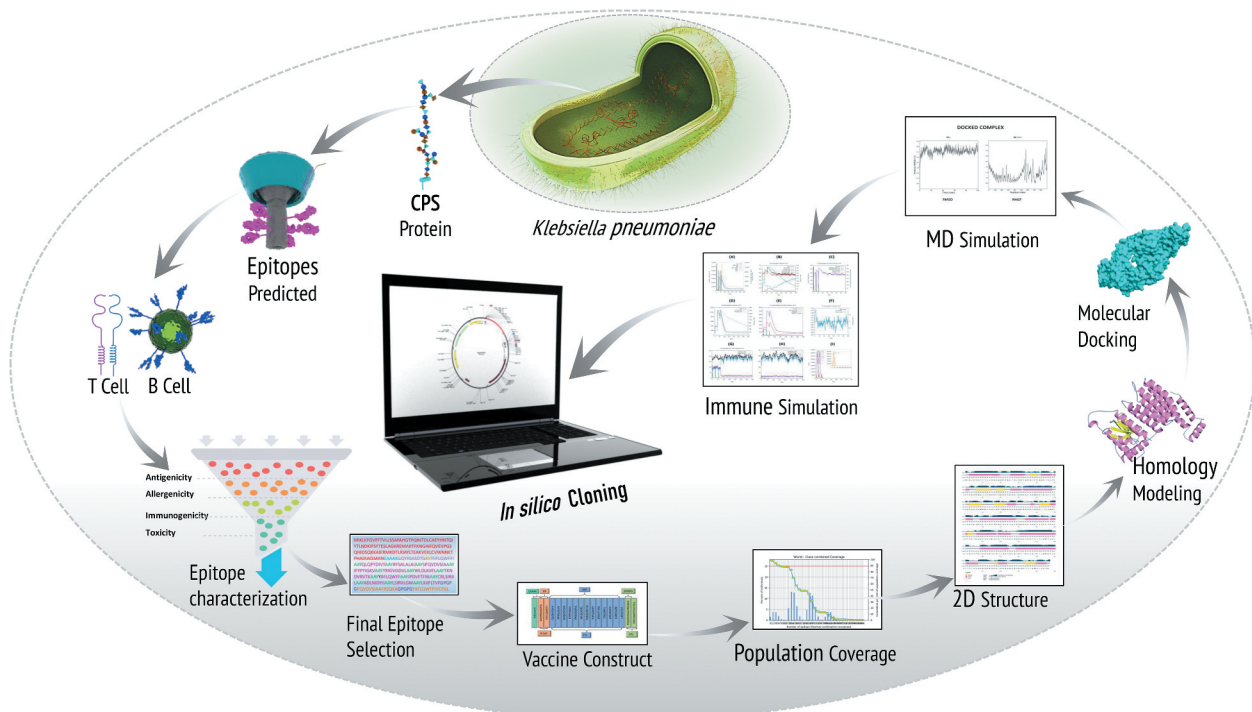


Figure 1. Workflow employed for the vaccine design.

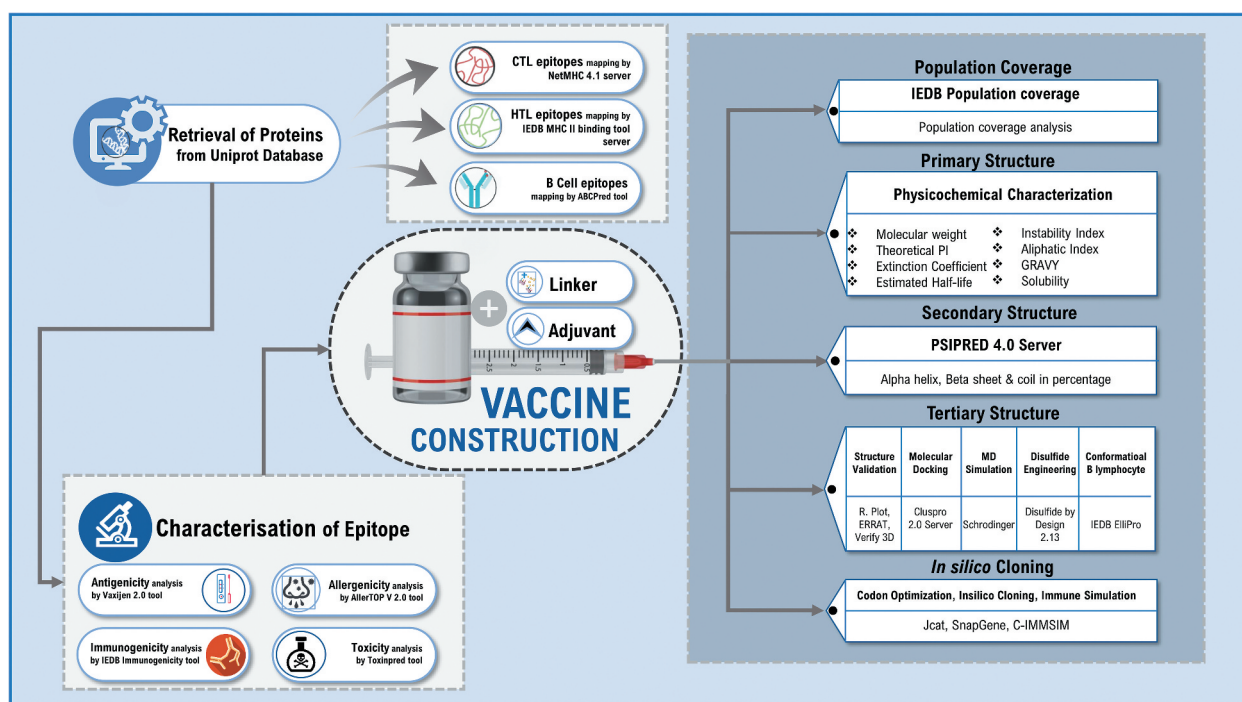


Figure 2. Schematic representation of the methodology for the development of multi-epitope vaccine against pneumonia fever.

to the human leukocyte antigen (HLA) [16] class I (recognizes CD8+ T cells), and class II (recognizes CD4 + T-cells) alleles [17]. Unlike protein or glycoprotein antigens, which elicit T-cell dependent antibody responses, polysaccharide antigens induce T-cell independent antibody responses [18].

### 2.2.1. CTL epitopes mapping

Identification of cytotoxic T lymphocyte (CTL) epitopes is a crucial step in epitope-driven vaccine design as MHC class I restricted CTL plays a critical role in controlling bacterial infections. The HLA class I molecules typically bind peptides 8–12 amino acids (mainly 9 amino acids) in length [19]. Due to the importance of T-cell epitopes, the Artificial Neural Networks NetMHC pan 4.1 server was used for the prediction of cytotoxic T-lymphocyte (CTL) epitopes derived from the protein sequence. The NetMHCpan4.1 (<http://www.cbs.dtu.dk/services/NetMHCpan/>), NetCTL 1.2 (<http://www.cbs.dtu.dk/services/NetCTL/>), and IEDB MHC class I processing predictions (<http://tools.iedb.org/processing/>) can predict human CTL epitopes in any given protein. The NetMHCpan4.1 server (<http://www.cbs.dtu.dk/services/NetMHCpan/>) can predict human CTL epitopes in any given protein. The NetMHCpan4.1 server can predict CD8<sup>+</sup> T-cell epitopes for 12 supertypes such as A1, A2, A3, A24, A26, B7, B8, B27, B39, B44, B58, and B62. We identified epitopes showing binding affinity for all the 12 supertypes. In this study, the threshold value for strong binder was 0.5%; while for weak binder was 2%, respectively. Sort by prediction score was selected for analysis. NetCTL1.2 server's predictions were based on peptide binding to MHC-I, proteasomal C-terminus cleavage score, and transport efficiency of Transporter Associated with Antigen Processing (TAP). Weight matrix was used to calculate the efficacy of the TAP transporter. The threshold set for the prediction of CTL epitopes was

0.75. The best candidates were further evaluated in IEDB MHC-I binding prediction tool.

### 2.2.2. HTL epitopes mapping

The selected protein was submitted to IEDB MHC-II binding tool (<http://tools.iedb.org/mhcii/>) for 15-mer Helper T lymphocyte (HTL) epitope prediction [20] and their respective-binding alleles using the CONSENSUS method [21] considering human HLAs as a reference set by default. Twenty-seven human leukocyte antigens (HLA) were evaluated. The percentile rank threshold of  $\leq 2$  was used here to ensure accuracy. The server assigns IC50 values to the predicted epitopes, which are inversely related to the binding affinity toward the MHC-II. IC50 scores of  $< 50$  represent a high binding affinity. The IC50 value  $< 500$  nM corresponds to intermediate binding affinity; however,  $< 5000$  nM is related to the low binding affinity of epitopes toward MHC-II. The binding affinity of predicted epitopes toward the MHC-II is inversely related to the percentile rank. The lowest consensus scores of the peptides were chosen to be the best binders as according to the IEDB server, a lower percentile rank indicates higher affinity. The best candidates were further evaluated on NetMHCIIpan4.0 (<http://www.cbs.dtu.dk/services/NetMHCIIpan/>) server. NetMHCIIpan 4.0 server is a state-of-the-art method for the quantitative prediction of peptide binding to MHC class II molecule of known sequence. The parameters were set at default.

### 2.3. Prediction of linear B-cell epitopes

Receptors present in the B-lymphocytes surface recognize and bind B cell epitopes. B-cell epitopes are essential in adaptive immunity and thus may be a key component in vaccine



development. There are two types of B-cell epitopes, namely, linear, and conformational epitopes [22]. ABCpred (<http://www.imtech.res.in/raghava/abcpred/>) and BCPREDS (<http://ailab-projects1.ist.psu.edu:8080/bcpred/predict.html>) servers were employed for Linear B Lymphocytes prediction. ABCpred server (<http://www.imtech.res.in/raghava/abcpred/>) was employed for linear B Lymphocytes prediction. ABCPred is a consistent algorithm-based webserver specifically used for the appropriate prediction of linear B-cell epitopes. As the B-cell epitope is present on the cell surface, exomembrane topology is considered as one of the essential parameters. The server specificity is 0.75, whereas the threshold of 0.51 (default threshold) and window length of 10 were set. BCPREDS uses a technique that employs the kernel method for the prediction of linear B cell epitopes. Kernel methods consist of different algorithms used for pattern analysis, a well-known member of this group is SVM (support vector machine). The prediction and output performance of BCPred (AUC = 0.758) is based on the SVM along with the employment of AAP (Amino acid pair antigenicity) (AUC = 0.7) [23]. The AAP is used for the prediction of linear B cell epitopes. Also, the B-cell epitopes were aligned with their whole-protein structure using PyMOL visualization tool.

#### 2.4. Characterization of screened epitopes

To validate and facilitate further refinement of predicted epitopes (B cell and T cell), vaccine protein prediction tool 'VaxiJen' v2.0 (<http://www.ddg-pharmfac.net/vaxijen/VaxiJen/VaxiJen.html>) was used at 0.4 thresholds for ensuring vaccine properties of target epitopes. The prediction of potential allergenicity is an important step in safety assessment as proteins and polypeptides have significant roles in inducing allergic reactions. The allergenicity of the selected epitopes was calculated by AllerTOP v2.0 (<https://www.ddg-pharmfac.net/AllerTOP/>). The amino acid sequences of CPS proteins were entered into the program separately and other parameters remained as defaults. AllerTOP uses the "k Nearest Neighbors (kNN)" method that distinguishes between allergenic and non-allergenic proteins through the route of exposure based on three nearest neighbors of known allergens with the highest accuracy (88.7%) as compared to several servers for allergen prediction. The ToxinPred tool was used to verify the linear peptides' toxicity as well as their other properties i.e. net molecular weight, SVM score, charge, hydrophilicity, and hydrophobicity [24]. And for the immunogenicity score, IEDB class I immunogenicity tool (<http://tools.iedb.org/immunogenicity/>) was utilized. It predicts the immunogenicity of an Epitope-MHC complex by analyzing the location and properties of amino acids.

#### 2.5. HLA peptide Docking

To quantify HLA-peptide binding efficiency as a part of the vaccine design, the epitopes were docked into their respective human leukocyte antigen (HLA) binding alleles. The basis of selection of the HLAs concerning the HLA-peptide docking was based on the strong binding affinity of the final selected CTL and HTL epitopes. PEP-FOLD v3.0 server, available at

<https://bioserv.rpbs.univ-paris-diderot.fr/services/PEP-FOLD3/>, was used to model the chosen CTL and HTL epitopes using the sOPEP sorting scheme with 200 simulations. This site uses the Forward Backtrack/Taboo sampling technique to predict the conformations of short peptides (5–50 amino acids) [25]. HLA-A\*01:01, HLA-A\*03:01, HLA-B\*07:02, HLA-B\*27:05, HLA-A\*24:02, HLA-B\*08:01, and HLA-B\*39:01 were chosen for CTL epitopes, while HLA-DRB1\*15:01, and HLA-DPB1\*04:02 were chosen for HTL epitopes. The RCSB Protein Data Bank (<https://www.rcsb.org/>) was used to get the structures of HLA alleles with co-crystallized ligands and then prepare the structures for docking by removing any ligands linked to them. AutoDock Vina was used to convert the PDB format of protein and ligand to PDBQT for molecular docking. Docking with AutoDock vina involves various steps such as molecule preparation and grid optimization that are carried out with the help of AutoDock Tools (ADT), a graphical user interface (GUI) employed by AutoDock [26]. Finally, using the AutoDock Vina software, a docking simulation was performed, and the findings were utilized as a benchmark for comparing the docking results of projected epitopes with similar parameters. The docked complex was visualized using the PyMOL Molecular Graphics System v2.2.3.

#### 2.6. Vaccine development

In the process of epitope selection, only peptides that were conserved across B and T cells, and that exhibited high antigenicity score, non-allergenic, nontoxicity, binding to the maximum number of HLA alleles were selected for further analysis. To construct the vaccine, antigenic epitopes were fused with the help of specific peptide linkers. In the next step, adjuvant was selected based on a literature study to develop the effectiveness of the vaccine. While choosing an adjuvant, characteristics such as hydrophilicity, hydrophobicity, hydrophobicity, isoelectric point (pI), and salvation were considered. One of the key issues with the design of peptide vaccine is its weak immunogenicity that can be resolved by designing a multi-epitope vaccine with appropriate adjuvant [27]. Additionally, the selected CTL, HTL, and B-cell epitopes were added to form a fusion peptide using KK, GPGPG, and AAY peptide linkers at specific positions. Adjuvant was attached to the linear B-cell epitopes with the help of the EAAAK linker. The linkers have a dual function, for the separation of epitopes to avoid neo-epitopes (junctional epitopes) formation and enhance the presentation of epitopes. Thus, linkers are helpful for differentiation and improvement of epitope presentation [28,29].

#### 2.7. Prediction of population coverage

MHC polymorphisms significantly vary at different frequencies in various ethnicities. The distribution and expression of HLA alleles vary by ethnicity and region around the world, influencing the development of an epitope-based vaccine for broad coverage [30]. We used the IEDB population coverage tool (<http://tools.iedb.org/population/>) for the analysis of the population coverage of the predicted epitopes and their respective HLA-binding alleles. By keeping the default parameters, 16 geographical areas such as East Asia, Northeast

Asia, South Asia, Southeast Asia, Southwest Asia, Europe, East Africa, West Africa, Central Africa, North Africa, South Africa, West Indies, North America, Central America, South America, and Oceania were selected for population coverage. Population coverage analysis was carried for combined HLA class I and class II.

### 2.8. Physicochemical features and secondary structural analysis

The physicochemical properties of the vaccine construct, including molecular weight (MW), theoretical isoelectric point (theoretical PI), instability index (II), aliphatic index (AI), and grand average of hydropathicity (GRAVY), *in vitro* and *in vivo* half-life were assessed using ProtParam server to assist experimental studies (<https://web.expasy.org/protparam/>). The instability index is one of the key parameters that are significantly considered as it helps in discarding the unstable protein candidates. Protein instability index greater than 40 is noted as unstable protein whereas a value less than 40 is considered as stable. The prediction of secondary structure was performed utilizing an online server PSIPRED available at <http://bioinf.cs.ucl.ac.uk/psipred/>. For the input, the primary amino acid sequences were entered. Position-specific iterated BLAST (Psi-Blast) was done to identify the related sequences and homology to the vaccine peptides [31]. This server uses a stringent cross-validation method which, for evaluating the performance of this method, PSIPRED 3.2 gives an average Q3 score of 81.6%, which is evaluated in CASP4. The processing of a position-specific scoring matrix was executed with the help of two feed-forward neural network which was attained from selected sequences. Finally, as an output, the secondary structure was calculated. Also, the prediction of the solubility of the designed vaccine was done with the SOLpro server (<http://scratch.proteomics.ics.uci.edu/>) [32], that predict using a two-stage SVM architecture and Protein-Sol server (<https://protein-sol.manchester.ac.uk/>) [33] with a 74% accuracy. SOLpro server is based on a suite of theoretical calculations and predictive algorithms for understanding protein solubility and stability.

### 2.9. Vaccine construct's antigenicity and allergenicity profiling

The antigenicity and allergenicity profiles of the vaccine construct were also determined. The VaxiJen server [34] was employed to assess the antigenicity of the vaccine construct, and the AllerTop server [35] was used to evaluate the non-allergenic nature of the vaccine construct.

### 2.10. Prediction of cytokine inducing epitopes

The development of different types of cytokines i.e. interferon-gamma (IFN- $\gamma$ ), and interleukin-10 (IL-10), and interleukin-17 (IL-17) I by MHC class II activated CD4 + T helper cells contribute significantly to infection control. Thus, the vaccine construct was also scanned for IFN- $\gamma$  inducing epitopes to analyze whether it can induce the IFN- $\gamma$  cells activation or not using IFN epitope server at (<http://crdd.osdd.net/raghava/ifnepitope/>) [36]. This software is based

on a dataset comprising of IFN-gamma inducing and non-inducing MHC class II binders through various approaches that have the maximum accuracy of 81.39% [36]. Our sequences were analyzed by motif and SVM hybrid and IFN-gamma versus non IFN-gamma. On the other hand, IL-10 and IL-17 inducing properties were predicted using IL10pred (<https://webs.iitd.edu.in/raghava/il10pred/algo.php>) and IL17eScan (<http://metagenomics.iiserb.ac.in/IL17eScan/>) web servers, respectively. The IL10pred and IL17eScan operations were carried out based on the SVM method and hybrid method, where the default threshold values were set at 0.2 and -0.3, respectively. All other parameters were kept as default.

### 2.11. Epitope conservancy analysis

In an epitope-based vaccine design, the use of conserved epitopes would likely provide wider protection across multiple strains, or even species, as compared to epitopes obtained from extremely variable genome regions. The epitope conservancy tool was designed to analyze the variability or conservation of epitopes. Epitope Conservancy Analysis of IEDB Analysis Resource (<http://tools.iedb.org/conservancy/>) computes the degree of the conservancy of an epitope within a given protein sequence set at a given identity level. 54 selected epitopes of the CPS protein across 20 *K. pneumoniae* strains showing high coverage from the population coverage analysis tool are selected and are given as plain text as input. Along with that protein sequence in FASTA format is also given by keeping other parameters as default. Further, the conservancy of the epitopic peptide region was also confirmed using the multiple expectation maximization for motif elicitation (MEME) utility (<http://meme.nbcr.net/meme3/meme.html>) program. The analysis was performed by keeping the number of repetitions: any; the maximum number of motifs: 10; maximum and minimum width: 20 and 6, respectively.

### 2.12. Determination and Validation of three-dimensional structure

The three-dimensional (3D) structure of the final multi-epitopic vaccine construct was constructed by using the ROBETTA server (<https://rosetta.bakerlab.org/>). The modeled structure was then visualized using the Pymol software. The modeled protein structure was validated using various web servers like PROCHECK (<https://servicesn.mbi.ucla.edu/PROCHECK/>) to find out the relative proportion of amino acids, which fall in the favored region of Ramachandran plot and are stereochemical accurate; VERIFY3D (<https://servicesn.mbi.ucla.edu/Verify3D/>) to determine the compatibility of an atomic model (3D) with its amino acid sequence; ERRAT (<https://servicesn.mbi.ucla.edu/ERRAT/>) to analyze the statistics of non-bonded interactions between different atom types and Verify 3D (<https://saves.mbi.ucla.edu/>) to find major geometrical aspects of protein structures.

### 2.13. Prediction of Discontinuous B- cell epitopes

To identify discontinuous B-cell epitopes in the modeled vaccine structure, we used the Ellipro tool (<http://tools.iedb.org/ellipro/>). Ellipro is a web-based tool on Thornton's method, the Jmol viewer and Modeler program, or a BLAST search of the Protein Data Bank. According to three algorithms, including PI value (Protrusion Index) that is an average value on epitopes' residues with higher solubility for higher PI, approximation of protein shape, and surrounding residues clustering based on the R group (in Å between two residues mass center), that determined larger epitopes with the larger R group. The default setting for the tool was i.e. 0.5 minimum score and 6 Å maximum distance. It predicts epitopes through an approximation of protein shape, residual protrusion index (PI), and neighbor residue clustering [37].

### 2.14. Disulfide engineering

Disulfide engineering is a novel approach for creating disulfide bonds into the target protein structure. Disulfide bonds are covalent interactions that help in increasing the protein stability along with the examination of protein interactions and dynamics [38,39]. Therefore, the selected refined vaccine model was subjected to the Disulfide by Design 2.12 [40] web platform to perform disulfide engineering. Initially, the refined protein model was uploaded and run for the residue pair search that can be used for the disulfide engineering purpose. Potential residue pairs were selected for mutations with cysteine residue using the 'create mutate function' of the Disulfide by Design 2.12 server (<http://cptweb.cpt.wayne.edu/DbD2/index.php>).

### 2.15. Docking between vaccine constructs and toll-like receptors

Toll-like receptors (TLR) are sensors recognizing molecular patterns of pathogens to initiate an innate immune system. It was demonstrated that TLR 2 is more susceptible to the Klebsiella family. Thus, the PDB file of TLR2 (PDB id: 3A7C) was obtained from Protein Data Bank (<http://www.rcsb.org/>), and then docking between the vaccine construct with TLR 2 was performed using the ClusPro server (<https://cluspro.bu.edu/>). ClusPro is based on PIPER, a Fast Fourier Transform (FFT) correlation approach for protein docking with pairwise interaction potential and uses three-step algorithms including 1) Rigid-body docking, 2) Cluster retained conformations, and 3) Refine by CHARMM minimization [41]. Each docking output had 30 models. Final analysis of the interactions between vaccine and TLR-2 was done using the Pymol software (<http://www.pymol.org>).

### 2.16. Molecular dynamics simulation

Molecular dynamics analysis is pivotal to demonstrate the stability of the modeled biomolecular structure. The stability of the complex (TLR-2 and Vaccine construct) was studied by Molecular dynamics simulations using

Gromacs2019 [42] using Charmm36-mar2019 force field for the protein parameters [43]. The complex was solvated explicitly using the TIP3P water model inside the cubic box, and its size extends 0.1 nm away from the protein on the edges of the box in each direction. The system's overall charge was neutralized by adding a 0.1 M salt concentration ( $\text{Na}^+\text{Cl}^-$ ). All the simulations were carried out in the GPU enabled Linux clusters. The entire system was minimized till the maximum force was less than 10 kJ/mol with the maximum steps of 50,000. The system was then equilibrated for 5ns under NVT conditions with temperature coupling for two separate groups and water-ions, at 300 K. Lincs algorithm is used to constrain the bonds of the hydrogen atoms [44]. Berendsen thermostat and V-rescale were used to keep the temperature and pressure constant, respectively. The cutoff distances for Coulomb and van der Waals interactions were set as 1.2 nm. Particle mesh Ewald method (PME) was used to calculate the long-range electrostatic interactions. The final production run was carried out for 100ns at a temperature of 300 K and a pressure of 1 bar. The results were analyzed using the gromacs modules and VMD [45], the graphs were generated using xmgrace.

### 2.17. Immune simulation for vaccine efficacy

To evaluate the immunogenic features of a multiepitope vaccination in real-life conditions, *in silico* immune simulations were performed using the C-ImmSim server (<http://150.146.2.1/CIMMSIM/index.php>). C-ImmSim is an agent-based dynamics simulator for immune reactions that uses the PSS matrix and machine learning approaches to predict the peptides and immunological interactions. The duration between doses 1 and 2 for vaccination should be at least 4 weeks. As a result, three injections containing one thousand vaccine proteins were administered 4 weeks apart at 1, 84, and 168 time-steps (each time-step equals 8 hours in real life, and time-step 1 is injection at time = 0), for a total of 1050 simulation steps (parameters were set in the C-ImmSim immune simulator). All of the remaining simulation settings were left at their default values. In addition, 3 injections of the chosen peptide were given four weeks apart to replicate recurring antigen exposure and investigate clonal selection in a typical endemic region. The Simpson index(D) is a measure of diversity that was calculated using the graph.

### 2.18. In silico cloning and codon optimization

To express the final multi-epitope vaccine in an appropriate expression vector that existed in the *E. coli* host, the reverse translation was carried out by Java Codon Adaptation Tool (JCat) (<http://www.jcat.de/>) and cDNA sequence was provided. The tool was used for performing the reverse transcription of the vaccine sequence, its codon optimization, and expression in the *E. coli* expression vector. The ideal value of the codon adaptation index (CAI) was found to be 1.0, calculated by the JCat tool. It also measures the vaccine insert's GC content, which

should range ideally between 30% and 70% to enhance the efficiency of transcription and translation. Also, using restriction enzymes, including, BamHI and EcoRI, cloning of the selected gene sequence from the final vaccine was performed. The optimized sequence of the multi-peptide vaccine was finally inserted into the expression vector pET-28a (+) utilizing the SnapGene tool (<https://www.snapgene.com/>).

### 3. Result

#### 3.1. Criteria for selection of final multi-epitope for vaccine construction

The vaccine needs to be antigenic, non-allergic in nature, and must induce humoral as well as cell-mediated immune responses against the targeted pathogen. Therefore, for the construction of an effective vaccine, the best epitopes were screened based on the criteria that they must be highly antigenic, non-allergenic, nontoxic, and must possess a good immunogenic score to evoke a strong immune reaction. Also, most importantly for a wider immunogenic response, only the common overlapping and conserved epitopes of the B-cell and T-cell that showed binding to the maximum number of HLA alleles were selected for the vaccine design.

Against this backdrop, antigenic probability was predicted by VaxiJen at <http://www.darrenflower.info/Vaxi-Jen/>, the first server for alignment-independent prediction of protective antigens. It was developed to allow antigen classification solely based on the physicochemical properties of proteins without recourse to sequence alignment [34]. The antigenicity of the epitopes was predicted at a 0.4% threshold for the bacterial model. Based on the prediction of the AllerTOP server, only non-allergen epitopes were selected for the vaccine construction. The toxicity, human similarity, and experimental records investigations were performed for

the selected linear epitopes. All peptides were predicted to be nontoxic by the Toxin pred tool. Hydrophobicity, hydrophilicity, and SVM score were also analyzed from the tool. IEDB immunogenicity server predicted the immunogenicity scores of all the epitopes. Epitopes having positive immunogenicity scores were considered for vaccine construction.

#### 3.2. Prediction of T-cell

##### 3.2.1. CTL epitopes mapping

The immune system is made up of a variety of cells and molecules that work together to remove foreign particles while maintaining cellular integrity. CTLs are CD8 + T cells that function in the recognition of foreign antigen fragments on MHC-I molecules and destroy target cells and thus protect both intracellular and extracellular infectious agents. CTL epitopes from the CPS protein were identified using the NetMHCpan 4.1, NetCTL 1.2, and IEDB MHC I server. Finally, based on the screening criteria, viz., highest antigenicity score, nontoxicity, and non-allergenicity, eight epitopes with respect to major HLA alleles (HLA-A\*01:01, HLA-A\*03:01, HLA-A\*24:02, HLA-B\*07:02, HLA-B\*27:05, HLA-B\*40:01, HLA-B\*58:01, HLA-B\*15:01, HLA-A\*01:01, HLA-A\*24:02, HLA-B\*07:02, HLA-B\*08:01, HLA-B\*39:01) were selected from both the proteins (Supplementary Table 1). Table 1 represents the selected MHC-I epitopes with respective MHC alleles, conservancy prediction, and average rank scores.

##### 3.2.2. HTL epitopes mapping

The Helper T-lymphocytes (HTLs) play a key role in adaptive immunity. They activate the B-cell, macrophages, and even the cytotoxic T-cells for the production of antibodies and eventually killing infected/damaged cells. The HTL epitopes were predicted using the IEDB MHCII server. The cutoff criterion was set to IC50 values < 50 nM and the percentile rank was ≤1. The best epitope candidates were again evaluated on the NetMHCIIpan4.0 server. Out of

**Table 1.** Predicted CTL epitopes from *Klebsiella pneumoniae* CPS proteins to design multi-epitope vaccine construct with their corresponding MHC Class I alleles and their immunogenic properties. Further details of the physicochemical parameters like hydrophobicity, hydrophilicity, charge and molecular weight of each epitope can be found in Supplementary Table 1. Please note that all the epitopes were found to be nontoxic and 100% conservancy as predicted by ToxinPred and IEDB Epitope Conservancy tool, respectively.

Uniprot_ID	CTL Epitope	Number of HLA binding alleles*	Position	Score	Conserved Across	Antigenicity Score
B5XT46	WLDLKIIFL	12	445	1.795	B-Cell, HTL	1.4777
	TKNDVVRVTK	12	344	3.185	HTL	1.7101
	IPDVFTFNI	12	238	1.416	B-Cell	1.8699
	CRLSIRIIL	12	126	0.299	HTL	1.7456
H2CZH6	QLQPYDIVY	12	333	0.375	HTL	1.0316
	RFSALALAI	12	7	1.251	HTL	0.8190
	IFYPYIGKV	12	126	4.228	B-Cell, HTL	0.6265
	YRIGVGDVL	12	85	0.014	B-Cell, HTL	0.9444

\*Please refer to Supplementary Table 1 for specific names of the HLA alleles.

**Table 2.** Predicted HTL epitopes from *Klebsiella pneumoniae* CPS protein to design multi-epitope vaccine construct with their corresponding MHC class II alleles and their immunogenic properties. Further details of the physicochemical parameters like hydrophobicity, hydrophilicity, charge, and molecular weight of each epitope can be found in Supplementary Table 2. Please note that all the epitopes were found to be nontoxic and 100% conservancy as predicted by toxinpred and IEDB epitope conservancy tool, respectively.

Uniprot_ID	MHC II Epitope	Number of HLA binding alleles*	Pos	IC50 value	Percentile_Rank	Conserved Across	Antigenicity Score
B5XT46	RIEDVVVSSIILLI	39	276–290	21	0.29	B-Cell, CTL	1.1092
H2CZH6	PQVDVSIAAFRSQKA	37	159–173	67	1.2	CTL	0.7756

\*Please refer to Supplementary Table 1 for specific names of the HLA alleles.



twenty-seven epitopes identified (Supplementary Table 2), based on antigenicity score, allergenicity, and binding affinity to the maximum number of HLA alleles as predicted by the IEDB MHCII tool, finally, two HTL epitopes of 15mer in length (RIEDVVVSSIILLI and PQVDVSIAAFRSQKA) were selected from both the capsular proteins as shown in Table 2.

### 3.3. Prediction of linear B-cell epitopes

Antigenic determinants recognized by B-cells are important because they can induce the immune system of an organism by producing antibodies. Continuous B-cell epitopes were predicted by the ABCpred server using a threshold of 0.51% and BCPREDS with a threshold of 75% as shown in the supplementary Table 3. Out of many B cell epitopes identified using the server, many of them were found to be toxic or allergenic, hence were not considered for further analysis. Further, few epitopes showed conservancy with the already selected T cell epitopes, hence were not selected to remove redundancy. Out of the twenty-five predicted epitopes, two unique linear epitopes (YIIFLQWFFI, GQYRSASDTG) were predicted from both the capsular polysaccharide-proteins based on the above-mentioned criteria as listed in Table 3. We have also aligned the B cell epitopes with the whole protein structures to ensure epitope recognition. Additionally, the B-cell epitopes are highlighted in yellow in Supplementary Figure 1. The root-mean-square deviation (RMSD) between the main chain atoms of the superimposed structure was observed to be 2.805Angstrom, which depicts stability of the structure.

### 3.4. HLA peptide docking

AutoDock Vina predicted the peptide–allele interaction affinities. The binding affinity of the CTL epitopes and their associated alleles was ranged between  $-6.0$  and  $-8.5$ , as shown in Table 4. The binding affinity of HTL epitopes was determined to be between  $-6.0$  and  $-6.5$ . (Table 4). In addition, the amino acid residues involved in hydrogen bond interactions were examined and are included in Table 4. Based on the docking score, Figure 3 depicts the CTL (WLDLKIIFL, TKNDVRVTK, IPDVFTFNI, CRLSIRIIL, QLQPYDIVY, RFSALALAI, IFYPYIGKV, and YRIGVGDVL) and HTL (RIEDVVVSSIILLI, and PQVDVSIAAFRSQKA) epitopes.

### 3.5. Vaccine development

To reduce the length of the vaccine construct, only overlapping epitopes having common B cell and CTL and HTL epitopes were taken into account. The vaccine construct was designed by combining the final selected two B-cell epitopes, 13 CTL epitopes, and two HTL epitopes using the linkers. Additionally, to improve the immunogenicity of the multi-epitope vaccine, the construct was tagged *in silico* with an adjuvant, cholera toxin B (CTB) (UniProt id: P01556) of amino

**Table 3.** Final selected B-cell epitopes from *Klebsiella pneumoniae* CPS protein and their corresponding immunogenic properties. Further details of the physicochemical parameters like hydrophobicity, hydrophaticity, hydrophilicity, charge, and molecular weight of each epitope can be found in Supplementary Table 3. Please note that all the epitopes were found to be nontoxic and 100% conservancy as predicted by toxinpred and iedb epitope conservancy tool, respectively.

Uniprot_ID	B-Cell Epitope	Position	Score	Conserved Across	Antigenicity Score
B5XT46	YIIFLQWFFI	109	0.77	CTL, HTL	3.8246
H2CZH6	GQYRSASDTG	108	0.77	CTL, HTL	1.0836

acid length 124 at the N-terminal region, which enhances the natural immune response [46]. The lack of toxicity combined with the stability and relative ease to express CTB either by its own or fused to peptides or proteins has made CTB an adjuvant easy to handle [47]. Therefore, the adjuvant was linked to the B cell with the EAAAK linker, whereas the B-cells are connected to each other with the help of the KK linker. Further, CTL and HTL epitopes are fused by AAY and GPGPG linkers, respectively. The schematic diagram of the vaccine construct is shown in Figure 4.

### 3.6. Prediction of population coverage of the vaccine construct

As different MHC-I and MHC-II HLA alleles are exposed at different frequencies (population/individual) in different ethnicities around the world, a frequency distribution analysis, or an analysis of how many individuals will be covered by the respective HLA alleles of the predicted epitopes, is an important part of developing an effective vaccine. The population coverage of the selected T cell epitopes was analyzed using the IEDB population coverage analysis tool. The results indicated that the vaccine is potential to elicit an immune response in 99.11% percentage of the world population, particularly highest in West Africa (99.92%), East Africa (99.68%), Europe (99.59%), Central Africa, and North America (99.57%) (Supplementary Table 4). It was noted that the population coverage rate exceeded 90% in almost all countries worldwide.

### 3.7. Physicochemical features and secondary structural analysis

According to the ExPASy ProtParam server results, the final multi-epitope vaccine with 287 amino acids was found to possess 31.25 kDa molecular weight (MW), and theoretical isoelectric point (PI) were calculated as 9.26. The total number of atoms was 4560 with an atomic composition, including Carbon (1482), Hydrogen (2300), Nitrogen (370), Oxygen (399), and Sulfur (7). Also, the total number of negatively charged residues (Aspartic acid + Glutamic acid) and positively charged residues (Arginine + Lysine) were calculated as 21 and 30, respectively. The estimated half-life was 30 hours in mammalian reticulocytes *in vitro*, more than 20 hours in yeast, and more than 10 hours in the *E. Coli in vivo*, respectively. Other properties such as instability index, aliphatic index, and grand

Table 4. The efficacy of the CTL and HTL epitopes to be used in vaccine construction.

MHC Type	Selected Epitopes	HLA binding allele	Binding affinity	Residues involved in hydrogen bond interaction
CTL	WLDLKIIFL	HLA-A*01:01	-6.0	THR73 – ILE6, TRP147 – TRP1, ARG114 – LEU2, ARG156 – ASP3
	TKNDVRVTK	HLA-A*03:01	-6.1	TRP147 – THR8, LYS146 – ARG6, THR80 – ARG6, LEU78 – LYS2, GLU19 – THR1, ARG82 – ASN3
	IPDVFTFNI	HLA-B*07:02	-8.2	TYR7 – ILE9, ARG62 – ASN8, GLU163 – ILE9
	CRLSIRIIL	HLA-B*27:05	-6.1	SER2 – ARG2, GLU264 – ARG2, TYR27 – ILE8
	QLQPYDIVY	HLA-A*01:01	-6.2	TYR113 – GLN1, SER2 – GLN1, SER4 – LEU2, GLU212 – TYR5, LYS243 – TYR9, GLU232 – TYR9
	RFSALALAI IFYPIYIGKV	HLA-A*24:02 HLA-B*08:01	-7.9 -8.5	ALA150 – ARG1, ASN77 – PHE2, TYR116 – SER3, THR73 – SER3, HIS70 – SER3, GLU63 – ILE9, TYR159 – ILE9, LYS66 – ALA8, LYS66 – ILE9 SER2 – TYR5, ASP29 – VAL9, SER4 – VAL9, SER4 – TYR5, SER4 – ILE6, ARG6 – ILE6, SER4 – ILE6, ARG6 – ILE6, ARG6 – GLY7, ARG6 – LYS8
HTL	YRIGVGDVL	HLA-B*39:01	-6.8	ARG97 – GLY6, ASN63 – TYR1, GLU166 – ARG2, THR163 – ARG2, THR163 – ILE3, THR163 – GLY4
	RIEDVWVSSIRILLI	HLA-DPB1*04:02	-6.0	THR141 – ARG1, TYR143 – ARG1, ALA11 – GLU3, ALA11 – VAL5, SER77 – SER9
	PQVDYSIAAFRSQKA	HLA-DRB1*15:01	-6.5	ASN69 – SER6, TYR13 – PRO1, THR113 – PRO1, THR113 – GLN2, ASN84 – ALA15, ILE82 – ALA15, TYR79 – ARG11

average of hydropathicity (GRAVY) were computed 30.19, 105.16, and 0.265. Therefore, it was determined that the vaccine is thermostable, soluble, and hydrophobic, naturally. Moreover, the solubility of the multi-epitope vaccine was calculated at 0.62 by the Solpro server of the Scratch protein predictor tool. Higher solubility of a protein stands for better purification during downstream processing; hence solubility is a major factor in post-production vaccine studies. The secondary structure of the protein results indicated 347 amino acid long construct involving 24.73% strands, 46.34% helices, and 28.91% random coils as represented in Figure 5. Higher proportions of alpha-helices would help in the maintenance of the stability of the vaccine protein's structure. The existence of random coils and strands in protein secondary structure corresponded with the potential of protein in the formation of antigenic epitopes (Supplementary Table 5). The overlapping epitopes are mostly located in random coil regions. It is reported that these regions are mainly located on the surface and could be formed as epitopes [48].

### 3.8. Vaccine's antigenicity and allergenicity profiling

In addition to assessing the antigenicity and allergenicity of individual epitopes, the final designed vaccine construct should be highly antigenic to stimulate a better immune response. Henceforth, the antigenicity of the whole vaccine construct was observed to be high with a score of 0.9422 as predicted by VaxigenV2.0, suggesting that the vaccine is immunogenic and can trigger a strong immune response. AllerTOPV2.0 tool also classified the construct to be non-allergen against humans.

### 3.9. Epitope conservancy analysis

Genomes of 20 *K. pneumonia* strains were mined to retrieve corresponding amino acid sequences of the CPS protein (Supplementary Table 6). Consequently, each of the shortlisted CTL, HTL, and B-cell epitopes were analyzed to study the conservancy across all strains using the Conservancy Analysis tool of IEDB (Supplementary Table 6). All selected epitopes demonstrated perfect 100% conservation (Tables 1–3). The results of the MEME tool corroborate the high conservancy of the epitopes as depicted by the sequence logo. The schematic representation of the conserved sequence logos is illustrated in Supplementary Figure 2.

### 3.10. Determination and Validation of three-dimensional structure

The three-dimensional structure of the final multi-epitope vaccine was modeled by using the Robetta server. Figure 6 depicts the developed final structure as visualized by the Pymol software. The quality of the predicted 3D model was assessed using various structure validation tools. The calculated Ramachandran plot using PROCHECK revealed that maximum residues fall in allowed regions, 92.2% in the most favored region, 7.4% additional allowed region, and 0.4% in the disallowed region, respectively. Further high scoring values in other structure validation tools, such as 85.37% in VERIFY3D and 99.27% in ERRAT,

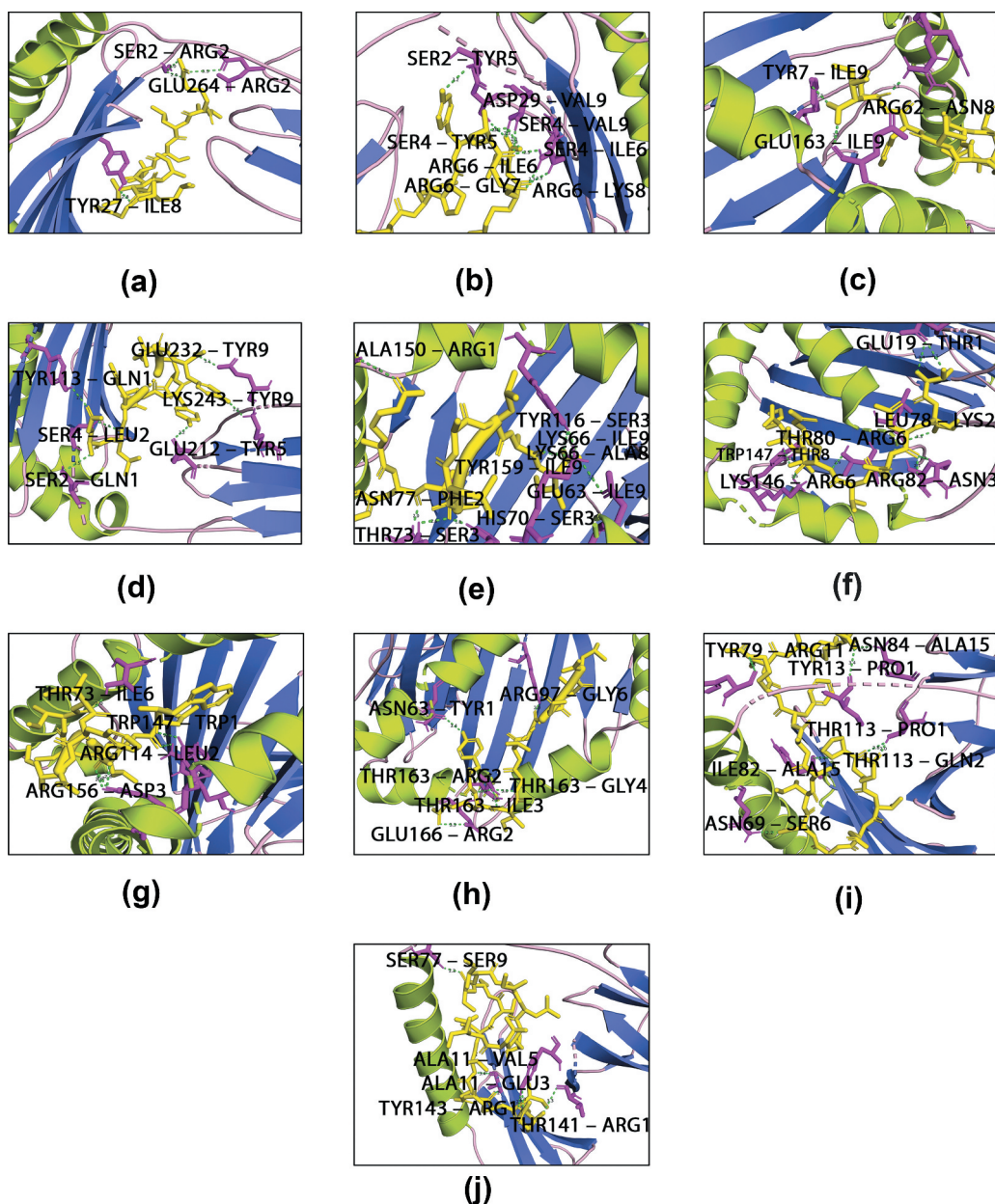


**Figure 3.** Molecular interaction between the predicted T-cell epitopes and their respective HLA binding alleles.

conclusively demonstrated the accuracy and reliability of the three-dimensional structure of the multi epitopic vaccine construct for further studies (Figure 7).

### 3.11. Prediction of discontinuous B-cell epitopes

Linear antibody epitopes could be predicted through sequence-based algorithms. In contrast, the prediction of discontinuous epitopes needs 3D structural information of the protein or polypeptide. Thus, the selected 3-D model was analyzed by the Ellipro server to predict potential discontinuous B-cell epitopes (Figure 8). Ellipro server identified four discontinuous B-cell epitopes. Supplementary Table 7 indicates residues, number of residues, and score of the B-cell epitopes in the designed construct.

### 3.12. Identification of cytokine inducing epitopes

The production of IFN- $\gamma$  contributes to the clearance of *K. pneumoniae* infections, especially for hypervirulent strains [49–51]. Therefore, the vaccine construct was also scanned for IFN- $\gamma$  epitopes. A total number of 55 positive IFN- $\gamma$  inducing epitopes with a score of greater than or equal to one were predicted from the vaccine sequence. The amino acid residues of the vaccine, which are located in the 124–139 region showed the highest score (Supplementary Table 8). It is reported in several studies that Interleukin-10 and Interleukin-17 play vital roles in host protection in the host defense against *K. pneumoniae* infections and in the septic response [52,53]. Therefore, the IL-10 and IL-17 inducing abilities of the HTL epitopes were evaluated. We found that two selected HTL epitopes were able to induce IL-10; whereas two



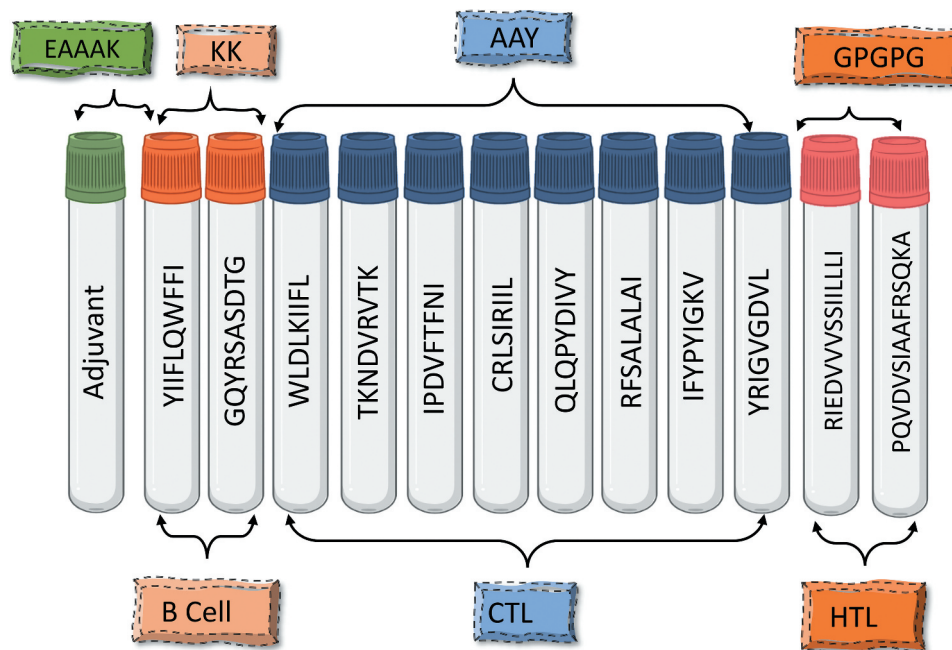


Figure 4. The structural arrangement of B and T-cell epitopes along with linkers and adjuvant for the final multi-epitope vaccine construct.

selected HTL epitopes were able to induce IL-17. Thus, the prioritized epitopes have the potential to produce more specific, efficient, safe, and robust immune responses as well as avoid all the undesired effects.

### 3.13. Disulfide bridging for vaccine protein stability

Disulfide by Design 2 server was used for disulfide engineering to increase the stability of the vaccine construct. A total of 55 pairs of residues were found that could be used for disulfide engineering, which is given in Supplementary Table 9. However, after evaluating other parameters such as energy and  $\chi_3$ , only a pair of residuals was finalized because their value falls below the allowable range, i.e., the value of energy should be less than 2.2 kcal/mol and  $\chi_3$  angle should be in between  $-87$  and  $+97$  degree [40]. Therefore, a total of three mutations were generated on the residue pairs, PHE9-ARG88, CYS30-CYS107, ALA260-SER280 for which the  $\chi_3$  angle and the energy were  $-86.78$  degree and 1.91 kcal/mol, respectively, as mentioned in Figure 9.

### 3.14. Docking between vaccine constructs and toll-like receptor-2

Toll-like receptors serve a vital role in the initiation of the inflammatory response by recognizing the pathogen. TLR2 contributes to the recognition of Klebsiella through interaction with bacterial lipoproteins, prevents detrimental overwhelming inflammation in the early stage of the infection, and also helps in antibacterial host defense at a late stage of the infection and/or upon exposure of the host to high bacterial numbers [54,55]. Many scientists have taken advantage of microbial-derived molecules to stimulate cells via TLR2, to exploit this ability in the development of vaccine adjuvants [56–58]. Hence, TLR 2 was chosen as the immune receptor and

obtained from the RCSB PDB database (PDB ID: 5YJB) while the vaccine model was used as a ligand. The protein–protein docking between the modeled vaccine construct and TLR-2 receptor was performed by the ClusPro server. The lowest energy level was estimated for the docked vaccine-TLR 2 complex is  $-1244.1$  and center energy between the ligand and receptor was noted as  $-1138.2$ . The hydrogen binding interacting residues in the vaccine-TLR2 docked complex were TYR159-ASP470, TYR159-ASN468, TYR159-ARG449, TYR163-ARG449, ASP276-ARG422, ASP276-GLN396, VAL278-GLN396, ARG263-GLU369, ARG263-GLU344, ARG263-ASN345, ALA261-LYS347, SER258-LYS347, ALA170-ARG400, PHE233-ARG400, ARG240-HIS398, ARG240-GLU374, ARG240-GLU375, TYR181-GLU374, ARG244-GLU375, ARG244-TYR376 with the distance of 2.1 Å, 2.1 Å, 2.4 Å, 2.0 Å, 2.1 Å, 1.9 Å, 1.9 Å, 1.9 Å, 1.9 Å, 1.9 Å, 1.7 Å, 1.8 Å, 1.9 Å, 1.7 Å, 2.1 Å, 1.8 Å, 1.9 Å, 2.0 Å, 1.8 Å, and 2.1 Å, respectively (Figure 10). Strong interactions between the designed construct and TLR 2 supports the hypothesis of *K. pneumoniae* susceptibility to TLR-2 like other Klebsiella families [59].

### 3.15. Molecular dynamics simulation

In order to gain insights into the dynamics of the vaccine construct with the receptors, molecular dynamics (MD) simulations were carried out. The simulation analysis was also important to validate the exposure of epitopes toward the host structure for the identification and handling of a substantial outcome. To accurately assess the stability and binding state of the ligand-receptor complexes, MD simulation was carried out on Gromacs 2019 for a total duration of 100 ns. The MD simulations took place in three different phases: system preparation, pre-processing, and production [60] with an assistant model building with Energy Refinement. The



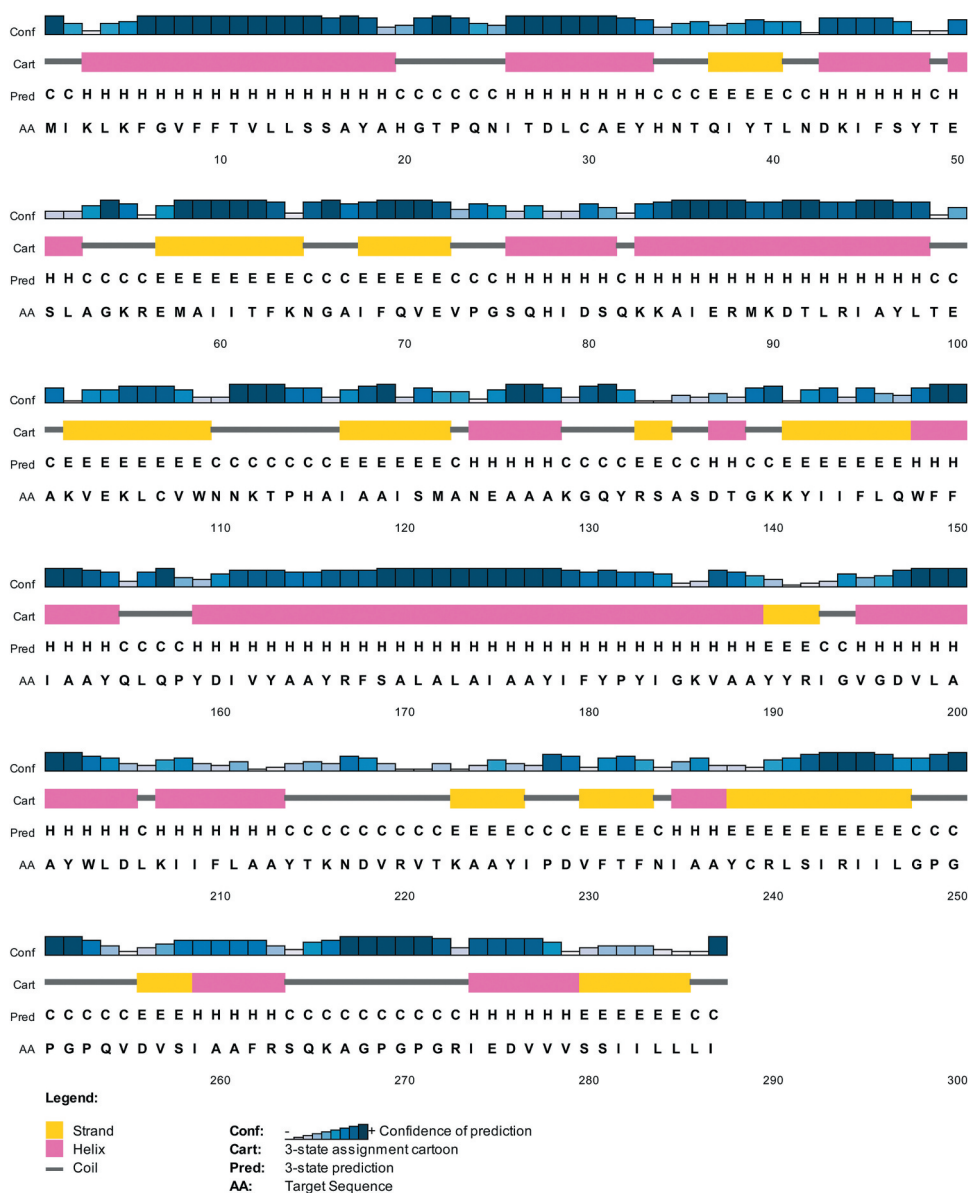


**Figure 5.** Secondary structure prediction of the final multi-epitope vaccine construct by using PSIPRED tool.

RMSDs and RMSFs were used to evaluate the most flexible parts of the target vaccine protein. The RMSD plot (Figure 11) reported that the system is at equilibrium and was fairly stable throughout the 100 ns simulation and seemed converging at the end, after 50 ns. The RMSD plot fluctuations were low thus indicating stable interaction between ligand (Vaccine model) and receptor (TLR 2). The most flexible regions of the vaccine molecule were also determined by analysis of MD simulation results. In this regard, the root-mean-square fluctuations (RMSF) of all residues of the vaccine-TLR2 complex were evaluated. The RMSF plot (Figure 11) showed maximum fluctuation in the range of residues between 290 and 330 which is the interacting loop of the protein with the ligand. The radius of gyration also assured the degree of compactness of the ligand-bound docked complex. It can be seen in Figure 11C that there was a lot of fluctuation during the initial portion of the simulation, but then it became stable, indicating that the

docked complex formed a more rigid conformation and therefore assured stability [61,62]. However, after 50 ns, the gyration in the structure began to stabilize at a value of around 3.3 nm throughout the remaining simulation time (Figure 11C). The stability of the interface in the TLR2-vaccine complex is defined by the calculation of hydrogen bonds between the TLR2 and vaccine in the complex during simulation. The study revealed that up to 60 ns, an average of 5 hydrogen bonds were maintained at the interface, increasing to 8 once the complex was stabilized (Figure 11D). The increase in hydrogen bonds indicates that the interface between TLR2 and the vaccine in the complex is becoming more stable. Analyzing the interface residues shows that several residues, particularly in the region between 300 and 450, in specific receptor residues R316, H318, Q321, F322, L324, N345, K347, F349, L371, Q396, H398, R400, T424, S445, R449 are well conserved in the interface before and after simulation.

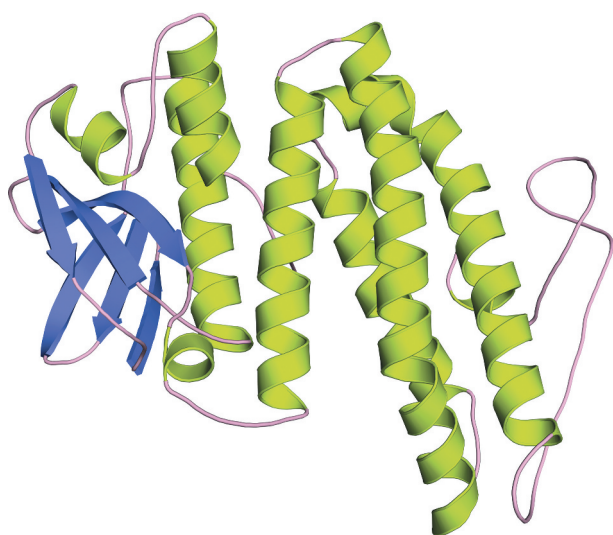


**Figure 6.** Homology modeling of the three-dimensional structure of the final multi-epitope vaccine construct.

Similarly, in the case of vaccine construct, the residues that were conserved in the interface with the receptor are Y163M T232, A236, C239, R240, I243, I246, L247, P251, P253, V255, V257, S258, I259, R263, and 278. As in the receptor case, the above residues of the vaccines are well conserved before and after the simulation. This analysis further illustrates the stability of the vaccine interaction with the receptor.

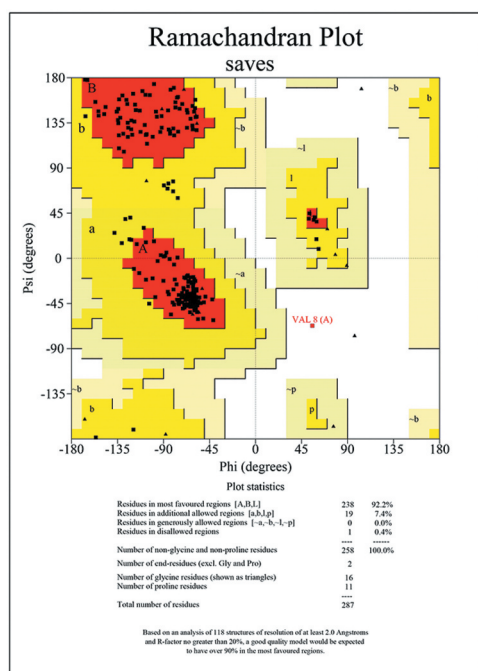
### 3.16. Immune simulation

C-ImmSim server was used to mimic the actual immune responses in the body upon exposure to the designed vaccine

construct. Usually, the primary immune response arises as a result of the first contact with an antigen and the first antibody produced is mainly IgM, although a small amount of IgG is also produced. As shown in Figure 12 the amount of the IgM significantly increased during the first injection of the vaccine construct (antigen) as a primary immune response. Secondary immune response occurs as a result of the second and subsequent exposure to the same antigen and is characterized by an increased level of IgM and IgG. Further, there was a noticeable increase in the level of IgM + IgG and decreased level of the antigen. Moreover, there was a striking increase in the level of IgM, IgG1 + IgG2, and IgG1 (Figure 12). These findings confirmed that the antibodies had a greater affinity to the vaccine construct (antigen) and would develop strong immune memory. Consequently, this resulted in increased clearance of the antigen upon subsequent exposures. Regarding the cytotoxic and helper T lymphocytes, high response in the cells populations with corresponding memory development was witnessed. Most importantly, the population of the Helper T lymphocytes remained higher during all exposure time. In the IFN- $\gamma$ -induced epitopes prediction, the results showed a high IFN- $\gamma$  concentration score compared to the other cytokines. The Simpson index D demonstrated the level of danger when the cytokines level increased which may result in complications during the immune response [63].

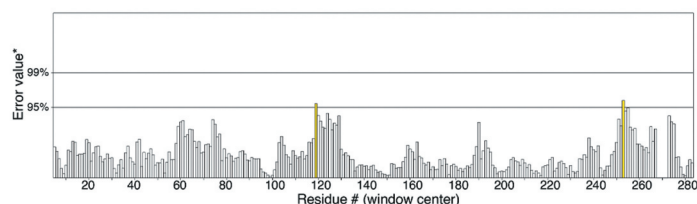
### 3.17. In silico cloning and codon optimization

The feasibility of cloning and expression of novel multi-epitope subunit vaccines in an appropriate expression vector is important. Thus, in order to analyze the cloning and expression efficiency of the developed vaccine construct in an expression vector, *in-silico* cloning was also carried out



### ERRAT RESULT

Overall quality factor\*: 99.270



### VERIFY 3D RESULT

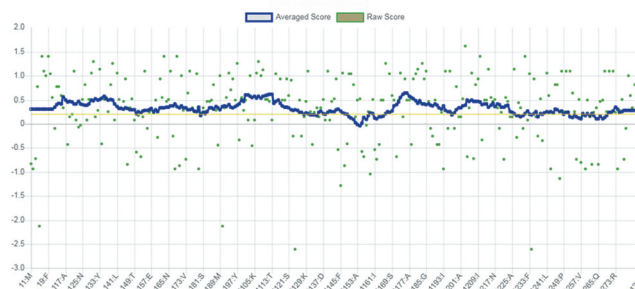


**Figure 7.** Developed multi-epitope vaccine structure validation results confirmed the model to be reliable and accurate.

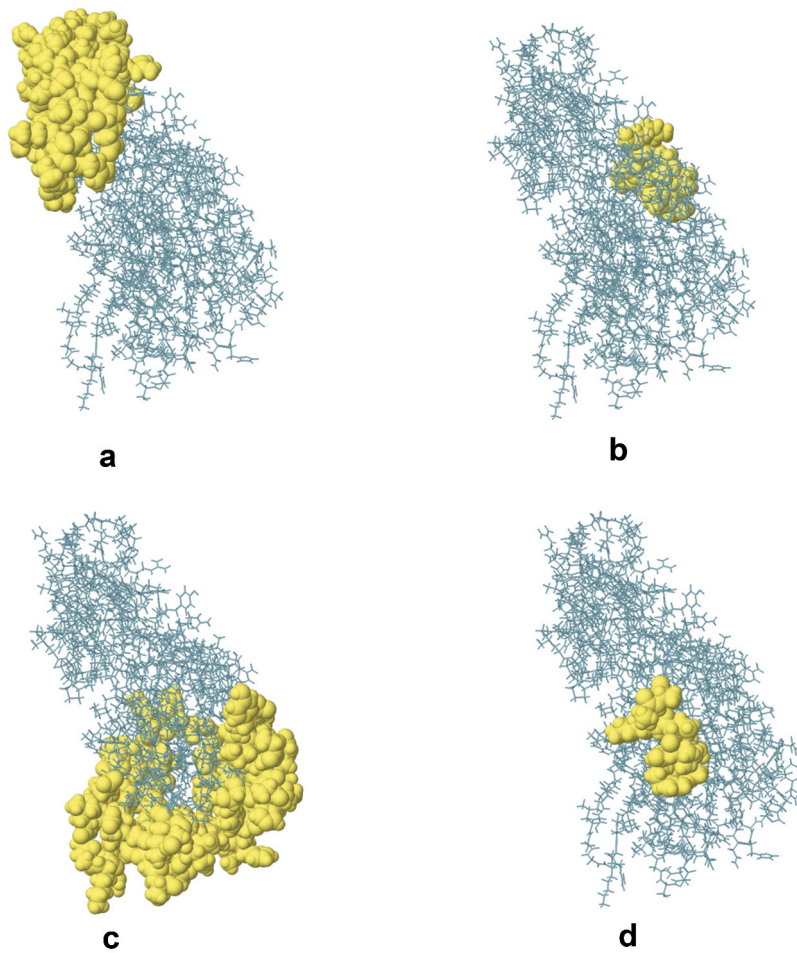


**Figure 8.** Developed multi-epitope vaccine structure validation results confirmed the model to be reliable and accurate. The conformational B-lymphocyte epitopes present in the vaccine. The yellow spheres showing epitopes containing (a) 56 residues (AA 182, AA 185–197, AA 242–281, and AA 284–285) with 0.784; (b) 10 residues (AA 124–133) with 0.777; (c) 72 residues (AA 16–25, AA 27–28, AA 30–40, AA 42–44, AA 46–47, AA 49–58, AA 60, AA 62–68, AA 70, AA 72–80, AA 82–83, AA 102, AA 109–115, and AA 155–160) with 0.691; (d) 8 residues (AA 215, AA 217 and AA 220–225) with 0.523.

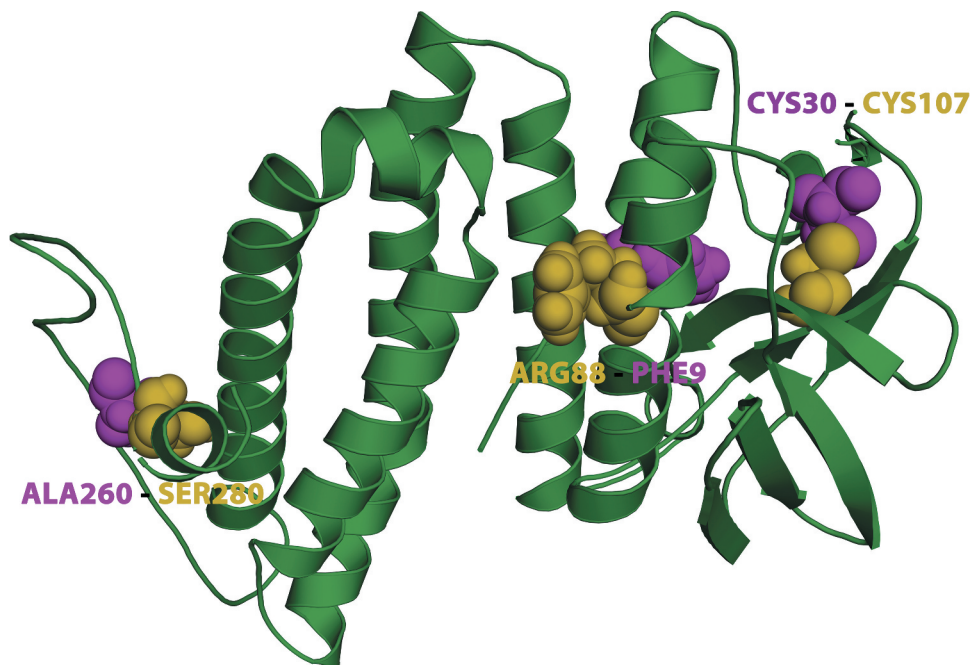


**Figure 9.** Disulfide engineering of the vaccine protein. Residue pairs showed in purple (PHE9, CYS30, ALA260) and olive green (ARG88, CYS107, SER280) spheres were mutated to cysteine residues to form disulfide bridge between them.

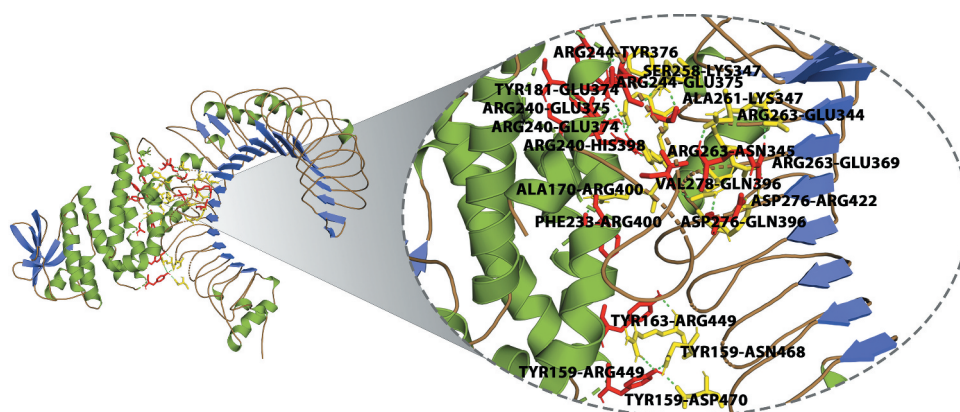


Figure 10. Molecular interaction of multi-epitope vaccine construct docked with TLR2.

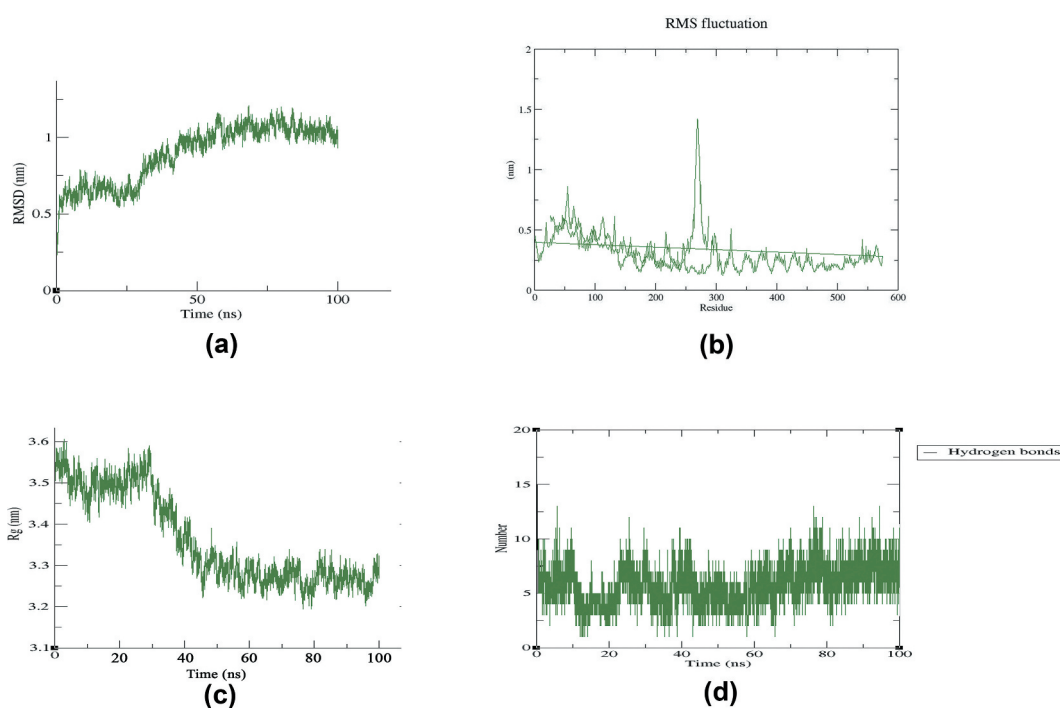


Figure 11. Root mean square deviation (RMSD) and root-mean-square fluctuation (RMSF) analysis of protein backbone and side chain residues of MD simulated vaccine construct.

using *E. coli* as a multi-epitope vaccine expression system. The optimization of the codon sequence was performed using Java Codon Adaptation Tool (JCat). Prokaryotic *E. coli* strain K12 was selected as the target organism and rho-independent transcription terminators, prokaryotic ribosome-binding sites and EaeI and StylI cleavage sites of restriction enzymes were avoided at the server. The codon adaptation index (CAI) and GC content revealed for the improved sequence are highly satisfactory with values of 0.97 and 49.59, respectively. The results suggest that the proposed vaccine construct possesses an efficient expression capability in the *E. coli* (host) expression vector. Also, 6x histidine was tagged to facilitate purification and solubilization of the vaccine protein after expression. Further, the

adapted codon sequence of the multi-epitope vaccine was inserted into the pET28a (+) vector using the SnapGene tool, for restriction cloning [64]. Finally, a plasmid map was generated with a sequence length of 6230 base pairs as shown in Figure 13.

#### 4. Discussion

*Klebsiella pneumoniae* has emerged as an urgent public health threat in many industrialized countries worldwide. Infections caused by *K. pneumoniae* are difficult to treat because these organisms are typically resistant to multiple drugs, and the patients have significant co-morbidities. Given the dearth of new antibiotics and the recent incidence of multidrug-



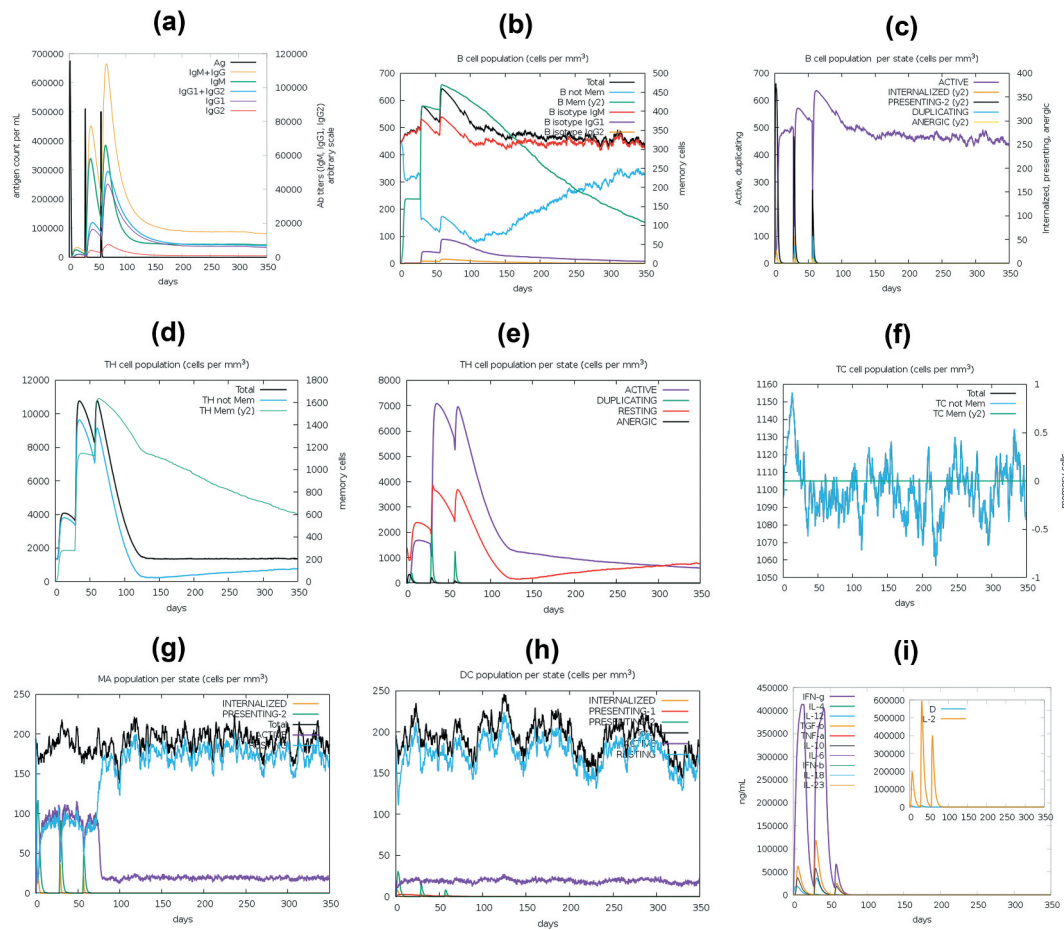


**Figure 12.** Immune response triggered by the designed vaccine. The graph shows (A) primary, secondary and tertiary immune responses, (B) B-cell population, (C) cytotoxic T-cell population, (D) helper T-cell population, (E) induction of cytokines and interleukins, (F) th1 mediated immune response, (G) macrophage population per state, and (H) dendritic cell population per state, and (I) production of cytokine and interleukins with simpson index (D) of immune response.

resistant strains, there is a critical need for the development of a vaccine against *K. pneumoniae* infections [20]. The capsule polysaccharide (CPS) of *K. pneumoniae* has long been viewed as an important virulence factor that promotes resistance to phagocytosis and serum bactericidal activity. Experimental studies have demonstrated that anti-CPS IgG isolated from human volunteers protects mice against *K. pneumoniae* sepsis [65]. In present times, the multi-epitope subunit vaccine is preferable than the traditional vaccine for several advantages including safety, higher stability, less allergic, autoimmune responses, and a more convenient production process. High throughput next-generation sequencing and advanced genomics and proteomics technologies have brought about a significant change in the computational immunology approach. With the abundance of genomic data and a plethora of immunoinformatics tools available, a better understanding of the immune response of the human body against a multitude of infectious pathogens can be deciphered [66].

In this study, novel T-cell (CTL and HTL) and B-cell epitopes from the antigenic CPS protein of *K. pneumoniae* were predicted as potential vaccine candidates. Utilizing different immunoinformatic tools, the screened epitopes were predicted to pose all desirable criteria for vaccine designing

including high immunogenicity, non-allergenicity, nontoxicity, stability, and conservancy. Docking analysis on these epitopes and their corresponding HLA alleles indicated that HLA-peptide interactions are energetically favorable. For the vaccine design, the LBL, CTL, and HTL epitopes were linked together with the help of KK, AAY, and GPGPG linkers, respectively. The CTB's amino acid sequence was also added as an adjuvant which was linked at the N-terminal of the construct with the help of the EAAK linker [67]. Physio-chemical properties were also determined for the vaccine using the ProtParam tool. The molecular weight of the vaccine was calculated to be 31.25 KDa that falls within the ideal range for a vaccine protein that is between 30 and 60 KDa; the theoretical PI of 9.26 indicates the basic nature of the vaccine, while an instability index score (30.19) indicated that the vaccine is stable [68]. The total numbers of negatively and positively charged residues were 21 and 30, respectively. Also, the multi-epitope vaccine provided solubility indexes greater than the average probabilities of the SOLpro server indicating the solubility of the vaccine construct. Interferon- $\gamma$  epitopes were even identified in the vaccine which confirmed the potential of vaccine to initiate Interferon- $\gamma$  exhibiting both immunomodulatory and immunostimulatory actions.

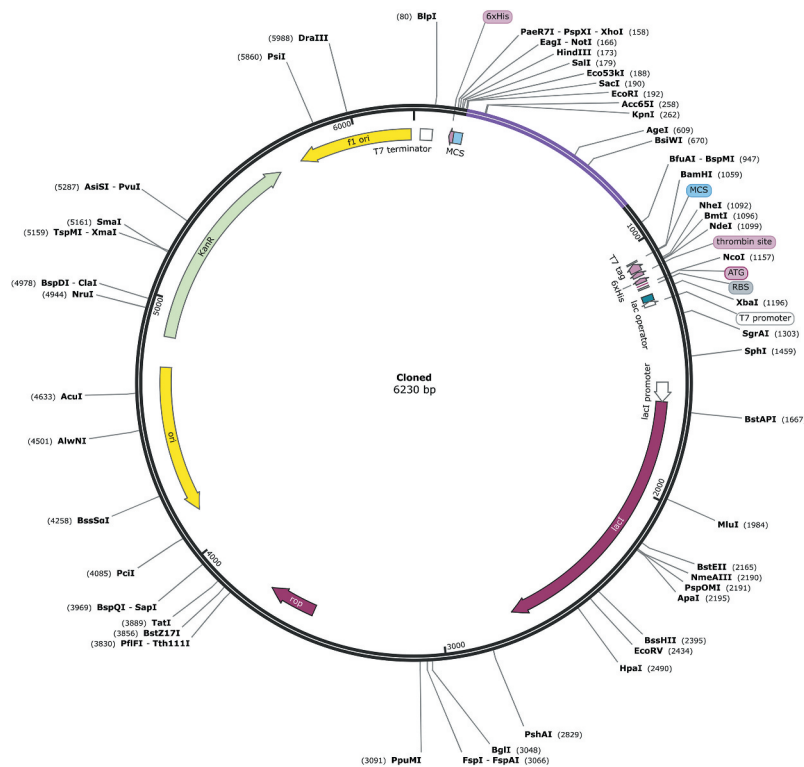


**Figure 13.** Restriction cloning of final multi-epitope vaccine by using the pET28a (+) expression vector in the *in silico* space. Black circle indicates the vector, and the purple part is the place where the vaccine is inserted.

Additionally, selected epitopes were observed to promiscuously bind with high affinity to the maximum number of HLA alleles thereby indicating that the vaccine construct elicits an immune response in approximately 99.11% of the world population coverage. As shown in Figure 5, the multi-epitope vaccine protein contains 46.34% (alpha helix), 24.73% (extended strand), and 28.91% (random coil). The secondary structure analysis revealed that a greater number of the alpha helices are present followed by the random coils and extended strands. The higher proportion of alpha-helices indicates the structural stability of the vaccine. Further, the presence of  $\alpha$ -helical coiled-coils peptides has been identified as significant 'structural antigens' types. When examined in synthetic peptides, these two structural types can fold into their native structure and therefore are recognized by antibodies naturally induced in response to infection [69].

In addition, the vaccine construct was found to express a high level of IFN- $\gamma$  epitopes indicating that the vaccine will promote antibacterial immunity, macrophage activation, and will enhance the antigen presentation [70]. Discontinuous B-cell epitopes prediction reported the presence of seven conformational epitopes that are specific for B-cell and can potentially elicit a humoral response [71]. Disulfide engineering is important for protein folding and stability. Also, structural disulfide engineering decreases the possible number of conformations for a given protein, resulting in decreased entropy and increased thermostability. In the developed vaccine construct, a total of three mutations were generated for which the  $\chi^3$  angle and the energy were  $-86.78$  degrees and 1.91 kcal/mol, respectively. Three-dimensional model of the

vaccine was constructed, and molecular dynamics simulation for 100 ns revealed a strong and stable binding affinity between the docked vaccine and toll-like receptor 2 (TLR2) molecule. It is reported that *K. pneumoniae* upregulates the expression of the TLR-2 [72]. Furthermore, immune simulation using the C-ImmSim server was performed to simulate the typical immune responses. Largely, there was a marked increase in the immunoglobulins coincided with the frequent injection of the vaccine construct. This result indicated the development of memory B cells. Additionally, the level of the active T cytotoxic and T helper lymphocytes was observed to escalate significantly supporting the enhancement of humoral and adaptive immune responses. The level of the IFN- $\gamma$  was also witnessed to remain high at peak level during the injection times. Finally, *in silico* cloning and codon optimization corroborated the feasibility of cloning and expression of the designed multi-epitope subunit vaccine construct.

## 5. Conclusion

The advancement of immuno-informatics tools in the post-genomic era enables us to facilitate the development of multi-epitope-based vaccines with higher accuracy and in a cost-effective manner. In this study, several immuno-informatics tools have been sequentially employed to find a novel multi-peptide vaccine candidate against *K. pneumoniae* infection. The highly antigenic, non-allergenic, and nontoxic as well as 100% conserved T-cell and B-cell epitopes were considered for final vaccine construction which would generate a high immunogenic response and at the same time does not cause any

harmful reaction within the body. Population coverage analysis showed that all potential T cell and B cell epitopes possess high population coverage percentages and could provide wider immune protection for worldwide regions. With high-cost requirements and multiple limitations for developing the live, attenuated, or inactivated vaccine preparation, these peptide-based vaccine candidates can be valuable candidates for diagnostic as well as for therapeutic and preventive vaccines and are useful for further experimental validation to prevent pneumonia disease.

## Acknowledgments

We acknowledge infrastructure support available through the DBT-BUILDER program (BT/INF/22/SP42155/2021) at KIIT Deemed to Be University, Bhubaneswar. We would like to thank Mr. Krishn Kumar Verma (Associate - Scientific Visualizer, KIIT-TBI) for his contribution in designing the graphical representation of figures.

## Reviewer disclosures

Peer reviewers on this manuscript have no relevant financial or other relationships to disclose.

## Author contributions

Conception and design: J Dey, SR Mahapatra, N Misra, M Suar; Computational work: J Dey, SR Mahapatra; Data Analysis and Curation: S Lata, S Patro; Original Draft Preparation: J Dey, SR Mahapatra, N Misra; Writing- Reviewing and Editing: N Misra, M Suar. The manuscript has been read and approved by all authors.

## Funding

This paper was not funded.

## Declaration of Interests

The authors have no relevant affiliations or financial involvement with any organization or entity with a financial interest in or financial conflict with the subject matter or materials discussed in the manuscript. This includes employment, consultancies, honoraria, stock ownership or options, expert testimony, grants or patents received or pending, or royalties.

## ORCID

Jyotirmayee Dey  <http://orcid.org/0000-0002-5543-7109>

Soumya Ranjan Mahapatra  <http://orcid.org/0000-0002-8927-458X>

Namrata Misra  <http://orcid.org/0000-0003-1813-6478>

## References

- Ullah SR, Majid M, Rashid MI, et al. Immunoinformatics driven prediction of multiepitopic vaccine against *Klebsiella pneumoniae* and mycobacterium tuberculosis coinfection and its validation via in silico expression. *Int J Pept Res Ther.* 2020;1–13. [10.1007/s10989-020-10144-1](https://doi.org/10.1007/s10989-020-10144-1).
- Rostamian M, Farasat A, ChegeneLorestani R, et al. Immunoinformatics and molecular dynamics studies to predict T-cell-specific epitopes of four *Klebsiella pneumoniae* fimbriae antigens. *J Biomol Struct Dyn.* 2020;1–11. [10.1080/07391102.2020.1810126](https://doi.org/10.1080/07391102.2020.1810126).
- Domingo-Calap P, Beamud B, Mora-Quilis L, et al. Isolation and characterization of two *Klebsiella pneumoniae* phages encoding divergent depolymerases. *Int J Mol Sci.* 2020;21(9):3160.
- Pichavant M, Delneste Y, Jeannin P, et al. Outer membrane protein A from *Klebsiella pneumoniae* activates bronchial epithelial cells: implication in neutrophil recruitment. *J Immunol.* 2003;171(12):6697–6705.
- Vuotto C, Longo F, Balice MP, et al. Antibiotic resistance related to biofilm formation in *Klebsiella pneumoniae*. *Pathogens.* 2014;3(3):743–758.
- Prestinaci F, Pezzotti P, Pantosti A. Antimicrobial resistance: a global multifaceted phenomenon. *Pathog Glob Health.* 2015;109(7):309–318.
- Woodford N, Turton JF, Livermore DM. Multiresistant gram-negative bacteria: the role of high-risk clones in the dissemination of antibiotic resistance. *FEMS Microbiol Rev.* 2011;35(5):736–755.
- Fleeman RM, Macias LA, Brodbelt JS, et al. Defining principles that influence antimicrobial peptide activity against capsulated *Klebsiella pneumoniae*. *Proc Natl Acad Sci U S A.* 2020;117(44):27620–27626.
- Tabassum R, Shafique M, Khawaja KA, et al. Complete genome analysis of a Siphoviridae phage TSK1 showing biofilm removal potential against *Klebsiella pneumoniae*. *Sci Rep.* 2018;8(1):1–11.
- Kim YK, Pai H, Lee HJ, et al. Bloodstream infections by extended-spectrum  $\beta$ -lactamase-producing *Escherichia coli* and *Klebsiella pneumoniae* in children: epidemiology and clinical outcome. *Antimicrob Agents Chemother.* 2002;46(5):1481–1491.
- March C, Cano V, Moranta D, et al. Role of bacterial surface structures on the interaction of *Klebsiella pneumoniae* with phagocytes. *PLoS One.* 2013;8(2):e56847.
- Martin RM, Bachman MA. Colonization, infection, and the accessory genome of *Klebsiella pneumoniae*. *Front Cell Infect Microbiol.* 2018;8:4.
- Sachdeva S, Palur RV, Sudhakar KU, et al. E. coli group 1 capsular polysaccharide exportation nanomachinery as a plausible antivirulence target in the perspective of emerging antimicrobial resistance. *Front Microbiol.* 2017;8:70.
- Tilocca B, Soggiu A, Greco V, et al. Immunoinformatic-based prediction of candidate epitopes for the diagnosis and control of paratuberculosis (John's disease). *Pathogens.* 2020;9(9):705.
- Tilocca B, Britti D, Urbani A, et al. Computational immune proteomics approach to target COVID-19. *J Proteome Res.* 2020;19(11):4233–4241.
- Kuhns JJ, Batalia MA, Yan S, et al. Poor binding of a HER-2/neu epitope (GP2) to HLA-A2.1 is due to a lack of interactions with the center of the peptide. *J Biol Chem.* 1999;274(51):36422–36427.
- Sakib MS, Islam M, Hasan AKM, et al. Prediction of epitope-based peptides for the utility of vaccine development from fusion and glycoprotein of nipah virus using in silico approach. *Adv Bioinformatics.* 2014;2014:402492.
- Opoku-Temeng C, Kobayashi SD, DeLeo FR. *Klebsiella pneumoniae* capsule polysaccharide as a target for therapeutics and vaccines. *Comput Struct Biotechnol J.* 2019;17:1360–1366.
- Tomita Y, Sato R, Ikeda T, et al. BCG vaccine may generate cross-reactive T cells against SARS-CoV-2: in silico analyses and a hypothesis. *Vaccine.* 2020;38(41):6352–6356.
- Wang P, Sidney J, Kim Y, et al. Peptide binding predictions for HLA DR, DP and DQ molecules. *BMC Bioinformatics.* 2010;11(1):1–12.
- Wang P, Sidney J, Dow C, et al. A systematic assessment of MHC class II peptide binding predictions and evaluation of a consensus approach. *PLoS Comput Biol.* 2008;4(4):e1000048.
- Zhang J, Jima D, Moffitt AB, et al. The genomic landscape of mantle cell lymphoma is related to the epigenetically determined chromatin state of normal B cells. *Blood.* 2014;123(19):2988–2996.
- EL-Manzalawy Y, Dobbs D, Honavar V. Predicting linear B-cell epitopes using string kernels. *J Mol Recognit.* 2008;21(4):243–255.
- Gupta S, Kapoor P, Chaudhary K, et al. & Open Source Drug Discovery Consortium. In silico approach for predicting toxicity of peptides and proteins. *PLoS One.* 2013;8(9):e73957.
- Lamiable A, Thévenet P, Tufféry P. A critical assessment of hidden markov model sub-optimal sampling strategies applied to the generation of peptide 3D models. *J Comput Chem.* 2016;37(21):2006–2016.

26. Trott O, Olson AJ. AutoDock vina: improving the speed and accuracy of docking with a new scoring function, efficient optimization, and multithreading. *J Comput Chem.* 2010;31(2):455–461.
27. Singh A, Thakur M, Sharma LK, et al. Designing a multi-epitope peptide based vaccine against SARS-CoV-2. *Sci Rep.* 2020;10(1):1–12.
28. Dorosti H, Eslami M, Negahdaripour M, et al. Vaccinomics approach for developing multi-epitope peptide pneumococcal vaccine. *J Biomol Struct Dyn.* 2019;37(13):3524–3535.
29. Saadi M, Karkhah A, Nouri HR. Development of a multi-epitope peptide vaccine inducing robust T cell responses against brucellosis using immunoinformatics based approaches. *Infect Genet Evol.* 2017;51:227–234.
30. Bui HH, Sidney J, Dinh K, et al. Predicting population coverage of T-cell epitope-based diagnostics and vaccines. *BMC Bioinformatics.* 2006;7(1):1–5.
31. Kaur H, Raghava GPS. Prediction of  $\beta$ -turns in proteins from multiple alignment using neural network. *Protein Sci.* 2003;12(3):627–634.
32. Magnan CN, Randall A, Baldi P. SOLpro: accurate sequence-based prediction of protein solubility. *Bioinformatics.* 2009;25(17):2200–2207.
33. Hebditch M, Carballo-Amador MA, Charonis S, et al. Protein-Sol: a web tool for predicting protein solubility from sequence. *Bioinformatics.* 2017;33(19):3098–3100.
34. Doytchinova IA, Flower DR. VaxiJen: a server for prediction of protective antigens, tumour antigens and subunit vaccines. *BMC Bioinformatics.* 2007;8(1):1–7.
35. Dimitrov I, Bangov I, Flower DR, et al. AllerTOP v. 2—a server for in silico prediction of allergens. *J Mol Model.* 2014;20(6):1–6.
36. Dhanda SK, Vir P, Raghava GP. Designing of interferon-gamma inducing MHC class-II binders. *Biol Direct.* 2013;8(1):1–15.
37. Ponomarenko J, Bui HH, Li W, et al. ElliPro: a new structure-based tool for the prediction of antibody epitopes. *BMC Bioinformatics.* 2008;9(1):1–8.
38. Khatoun N, Pandey RK, Prajapati VK, et al. Exploring Leishmania secretory proteins to design B and T cell multi-epitope subunit vaccine using immunoinformatics approach. *Sci Rep.* 2017;7(1):1–12.
39. Pandey RK, Bhatt TK, Prajapati VK, et al. Novel immunoinformatics approaches to design multi-epitope subunit vaccine for malaria by investigating anopheles salivary protein. *Sci Rep.* 2018;8(1):1–11.
40. Craig DB, Dombkowski AA, Kukla R. Disulfide by design 2.0: a web-based tool for disulfide engineering in proteins. *BMC Bioinformatics.* 2013;14(1):1–7.
41. Khairkhan N, Aghasadeghi MR, Namvar A, et al. Design of novel multi-epitope constructs-based peptide vaccine against the structural S, N and M proteins of human COVID-19 using immunoinformatics analysis. *PLoS One.* 2020;15(10):e0240577.
42. Abraham MJ, Murtola T, Schulz R, et al. GROMACS: high performance molecular simulations through multi-level parallelism from laptops to supercomputers. *SoftwareX.* 2015;1:19–25.
43. MacKerell AD, Bashford D, Bellott M, et al. All-atom empirical potential for molecular modeling and dynamics studies of proteins. *J Phys Chem B.* 1998;102(18):3586–3616.
44. Lemak AS, Balabaev NK. On the Berendsen thermostat. *Mol Simulat.* 1994;13(3):177–187.
45. Humphrey W, Dalke A, Schulten K. VMD: visual molecular dynamics. *J Mol Graph.* 1996;14(1):33–38.
46. Dar HA, Zaheer T, Shehroz M, et al. Immunoinformatics-aided design and evaluation of a potential multi-epitope vaccine against *Klebsiella pneumoniae*. *Vaccines (Basel).* 2019;7(3):88.
47. Stratmann T. Cholera toxin subunit B as adjuvant—an accelerator in protective immunity and a break in autoimmunity. *Vaccines (Basel).* 2015;3(3):579–596.
48. Li Y, Liu X, Zhu Y, et al. Bioinformatic prediction of epitopes in the emy162 antigen of *Echinococcus multilocularis*. *Exp Ther Med.* 2013;6(2):335–340.
49. Clemente AM, Castronovo G, Antonelli A, et al. Differential Th17 response induced by the two clades of the pandemic ST258 *Klebsiella pneumoniae* clonal lineages producing KPC-type carbapenemase. *PLoS One.* 2017;12(6):e0178847.
50. Lin YC, Lu MC, Lin C, et al. Activation of IFN- $\gamma$ /STAT/IRF-1 in hepatic responses to *Klebsiella pneumoniae* infection. *PLoS One.* 2013;8(11):e79961.
51. Moore TA, Perry ML, Getsoian AG, et al. Divergent role of gamma interferon in a murine model of pulmonary versus systemic *Klebsiella pneumoniae* infection. *Infect Immun.* 2002;70(11):6310–6318.
52. Yoshida K, Matsumoto T, Tateda K, et al. Induction of interleukin-10 and down-regulation of cytokine production by *Klebsiella pneumoniae* capsule in mice with pulmonary infection. *J Med Microbiol.* 2001;50(5):456–461.
53. Yang M, Meng F, Wang K, et al. Interleukin 17A as a good predictor of the severity of *Mycoplasma pneumoniae* pneumonia in children. *Sci Rep.* 2017;7(1):1–11.
54. Wieland CW, van Lieshout MH, Hoogendijk AJ, et al. Host defence during *Klebsiella pneumoniae* relies on haematopoietic-expressed toll-like receptors 4 and 2. *Eur Respir J.* 2011;37(4):848–857.
55. Jeon HY, Park JH, Park JI, et al. Cooperative interactions between toll-like receptor 2 and toll-like receptor 4 in murine *Klebsiella pneumoniae* infections. *J Microbiol Biotechnol.* 2017;27(8):1529–1538.
56. Oliviera Nascimento L, Massari P, Wetzler LM. The role of TLR2 in infection and immunity. *Front Immunol.* 2012;3:79.
57. Alam MM, Jang YS, Herrler G. Veterinary immunology: development of vaccines and diagnostic techniques. [10.1155/2014/619410](https://doi.org/10.1155/2014/619410)
58. Duthie MS, Windish HP, Fox CB, et al. Use of defined TLR ligands as adjuvants within human vaccines. *Immunol Rev.* 2011;239(1):178–196.
59. Bengoechea JA, Sa Pessoa J. *Klebsiella pneumoniae* infection biology: living to counteract host defences. *FEMS Microbiol Rev.* 2019;43(2):123–144.
60. Gajula MNVP, Kumar A, Ijaq J. Protocol for molecular dynamics simulations of proteins. *Biol Protoc.* 2016;6(23):e2051.
61. Azam SS, Uddin R, Wadood A. Structure and dynamics of alpha-glucosidase through molecular dynamics simulation studies. *J Mol Liq.* 2012;174:58–62.
62. Lobanov MY, Bogatyreva NS, Galzitskaya OV. Radius of gyration as an indicator of protein structure compactness. *Mol Biol (Mosk).* 2008;42(4):623–628.
63. Mahapatra SR, Dey J, Kushwaha GS, et al. Immunoinformatic approach employing modeling and simulation to design a novel vaccine construct targeting MDR efflux pumps to confer wide protection against typhoidal *Salmonella* serovars. *J Biomol Struct Dyn.* 2021;1–13. [10.1080/07391102.2021.1964600](https://doi.org/10.1080/07391102.2021.1964600).
64. Dey J, Mahapatra SR, Singh P, et al. B and T cell epitope-based peptides predicted from clumping factor protein of *Staphylococcus aureus* as vaccine targets. *Microb Pathog.* 2021;160:105171.
65. Cryz SJ, Fürer E, Germanier R. Protection against fatal *Klebsiella pneumoniae* burn wound sepsis by passive transfer of anticapsular polysaccharide. *Infect Immun.* 1984;45(1):139–142.
66. Purcell AW, McCluskey J, Rossjohn J. More than one reason to rethink the use of peptides in vaccine design. *Nat Rev Drug Discov.* 2007;6(5):404–414.
67. Mahapatra SR, Sahoo S, Dehury B, et al. Designing an efficient multi-epitope vaccine displaying interactions with diverse HLA molecules for an efficient humoral and cellular immune response to prevent COVID-19 infection. *Expert Rev Vaccines.* 2020;19(9):871–885.
68. Narang PK, Dey J, Mahapatra SR, et al. Functional annotation and sequence-structure characterization of a hypothetical protein putatively involved in carotenoid biosynthesis in microalgae. *S. Afr. J. Bot.* 2021;141:219–226.
69. Corradin G, Villard V, Kajava AV. Protein structure based strategies for antigen discovery and vaccine development against malaria and other pathogens. *Endocr Metab Immune Disord Drug Targets.* 2007;7(4):259–265.
70. Chatterjee R, Sahoo P, Mahapatra SR, et al. Development of a conserved chimeric vaccine for induction of strong immune response against *Staphylococcus aureus* using immunoinformatics approaches. *Vaccines (Basel).* 2021;9(9):1038.
71. Mahapatra SR, Dey J, Kaur T, et al. Immunoinformatics and molecular docking studies reveal a novel multi-epitope peptide vaccine against pneumonia infection. *Vaccine.* 2021;39(42):6221–6237.
72. Regueiro V, Moranta D, Campos MA, et al. *Klebsiella pneumoniae* increases the levels of toll-like receptors 2 and 4 in human airway epithelial cells. *Infect Immun.* 2009;77(2):714–724.